AD NUMBER

AD862065

NEW LIMITATION CHANGE

TO

Approved for public release, distribution unlimited

FROM

Distribution authorized to U.S. Gov't. agencies and their contractors; Critical Technology; AUG 1969. Other requests shall be referred to Commanding Officer, Naval Weapons Center, China Lake, CA 93555.

AUTHORITY

USNWC ltr, 30 Aug 1974

NWC TP 4779

YAWING MOTION OF 5"0 MK 41 PROJECTILE STUDIED BY MEANS OF YAW SONDES

by

W. R. Haseltine
Research Department

ABSTRACT. The 5"0 Mk 41 projectile was fired at both high and low muzzle velocities, and its oscillatory yawing motion studied by a telemetry technique. At high subsonic velocities this projectile develops a steady precessional motion of amplitude about 4 degrees. On a long flight, from high velocity launch, this behavior shows up late on the downward trajectory leg. The instability at small yaw and the limit cycle were found to be caused by a large and highly nonlinear Magnus moment. Aerodynamic coefficients were derived.

NAVAL WEAPONS CENTER
CHINA LAKE, CALIFORNIA • AUGUST 1969

78

NAVAL WEAPONS CENTER
AN ACTIVITY OF THE NAVAL MATERIAL COMMAND

M. R. Etheridge, Capt., USN ..... Commander
Thomas S. Amlie, Ph.D. ..... Technical Director

FOREWORD

This report presents final results of projectile stability experiments conducted during the years 1965 through 1968.

This work was supported initially by Independent Exploratory Development Task Assignment No. R361-00-000/216-1/F008-98-16 and continued on Naval Ordnance Systems Command Task Assignment Nos. ORD-035-101/200-1/UF008-09-01 and ORD-351-001/200-1/UF17-323-501.

This report is released at the working level and does not represent the official opinion of the Naval Weapons Center.

Released by
D. E. ZILMER, Head
Mathematics Division
28 July 1969

Under authority of
H. W. HUNTER, Head
Research Department

NWC Technical Publication 4779

Published by.....Research Department
Collation.....Cover, 25 leaves, DD Form 1473, abstract cards
First printing.....130 unnumbered copies
Security classification.....UNCLASSIFIED

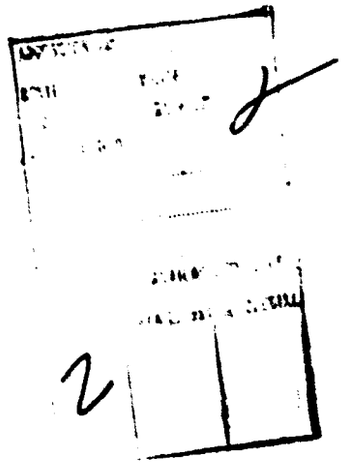

CONTENTS

ACKNOWLEDGMENT

The author wishes to acknowledge the valuable assistance of: R. K. Bucher in the conduct of the firings; P. W. Roper in modifying the sondes and preparing the projectiles; W. H. Allan for designing the sabot and help in charge establishment; and R. J. Stirton for supervising reduction of yaw sonde records.

THE PROBLEM

In the past fifteen years it has become evident that many spin-stabilized projectiles and rockets show symptoms of dynamic instability. While they are gyroscopically stable, and the yawing motion is oscillatory, the two modes of oscillation are not always damped. Over certain speed ranges either the fast mode, the nutation, or the slow mode, the precession, will grow from small amplitudes to larger instead of decaying away. Some otherwise promising designs have proved worthless for their intended purpose because of such behavior. Even among those missiles which are well enough behaved to have been adopted for service use, many, perhaps most, show an instability of the precession at high subsonic speeds, say between Mach numbers 0.7 and 1.0. Typically, as in the case of the 105-mm Shell, M1, the precession grows from a small size to an amplitude of a few degrees, and then stays in a limit cycle (Ref. 1). Worse behavior is also known.

A few years ago, when development of rocket-assisted ammunition for the Navy's 5"0 guns was undertaken, it became important to know whether the 5"0 Shell, Mk 41 (that for the 5"0/54 gun) showed any such behavior; first, because the very long flight times of RAP and the expected low ratio of spin to velocity late in flight should accentuate the pathology and its effects on range and dispersion; second, because existing spark range data (Ref. 2), though showing considerable scatter, indicated instability at high subsonic speeds. New spark range measurements were made by the Ballistic Research Laboratories and wind-tunnel measurements by the Naval Ordnance Laboratory, White Oak. These measurements and their significance are reviewed in Ref. 3. They confirm the indications in Ref. 2 that the Magnus moment coefficient at high subsonic speeds and very small yaw angles is such that undamping of the precession is to be expected. In addition, the wind-tunnel data indicate a change of sign of the Magnus moment at about 4 degrees yaw. Such a change points to the existence of a limit cycle.

It is plainly of great interest and importance to confirm the predicted behavior by experiments on real shell, observing the yawing behavior over whole trajectories. This is especially true since (a) the spark range experiments were limited in the number of speed and yaw amplitude combinations obtained, the values of the Magnus moment and the yaw damping coefficients scattered badly in the realm of interest, and there were insufficient data to even begin to deduce the functional form of the dependence on yaw angle; (b) wind-tunnel measurements of Magnus moment at small angles are extremely difficult and at the time

of Ref. 3 did not exist for this round below 4 degrees, and there are serious questions concerning the effects of Reynold's number and the supporting sting. What is needed is a device which will do for shell what the Solar Yaw Camera (Ref. 4, p. 405) did for rockets, and, if possible, easier.

Now even before the problem became acute for the 5"0/54, the British had announced (at the second meeting of Panel 07, TTCP, in 1963) that they had developed a Yaw Sonde with just the desired properties. Their government made a gift of a few sondes to this Station in 1964, and we later purchased more. Use of the sonde by its originators is described in Ref. 5. It was therefore decided to use these sondes to study the motion of the Mk 41 shell. Two groups of shots were planned. One group was to be fired with a muzzle velocity just above sonic, so that a long flight at speed between Mach No. 0.7 and 1.0 would be obtained, giving full opportunity to observe limit cycle behavior. The other group was to be fired at full service charge, and for maximum range, to check the theoretical prediction that the round would fly at small yaw until several seconds before impact, when a limit cycle in precession would develop. Later, these plans were extended to include tests of rounds without the rotating band, for the results reported in Ref. 6 suggested that decided changes might result. All records of yawing motion were to be fitted with theoretical curves calculated by a computer, so that values could be derived for the round's aerodynamic coefficients, including insofar as possible their functional dependence on yaw angle (see Ref. 7). It was hoped that this set of experiments would be the start of a series studying more generally Magnus instabilities of spinning projectiles and trying to find cures.

PRINCIPAL CONCLUSIONS

The 5"0 Shell Mk 41 does indeed exhibit a limit cycle in precession at Mach numbers between 0.7 and about 1.0. When it is fired at a velocity just above sonic, the small initial precession starts to increase almost at once, and then reaches a steady amplitude. In all but two of the nine cases available this amplitude was a little less than 4.0 degrees, and there is some doubt as to the significance of the two exceptions. The initial nutation is damped, at least at first, but may persist at small (1.0 deg or less) amplitude superimposed on the larger precession. When the shell is fired at about Mach 2.2 and a Q.E. of 45 deg., both precession and nutation are rapidly damped out to undetectable size. The flight time is about 74 sec, and at from 15 to 25 sec before impact small precessions become visible, which then grow steadily, but do not reach the 4.0-deg amplitude before impact. Nutations are invisible or nearly so during this time.

In the comparison of computed curves of orientation angle with the data from the sondes, very good fits were obtained to both frequency and amplitude of the precessions, and, when the data were of adequate quality to show nutations reliably, also to the frequency of these. It appears certain that from Mach number 0.70 to at least 0.95 and possibly 1.00, the Magnus moment coefficient K_T (or $-\pi/16\ C_{np\alpha}$) is positive and at least as large as 0.095, quite possibly as large as 0.150; and that it changes sign rather suddenly at 4.0 degrees or a little more total yaw angle, staying negative at least to 6.0 deg. Supersonically the value of K_T was assumed to be -0.024, and the fits are all relatively insensitive to moderate changes in this value. The yaw damping factor K_H $(-\pi/16\ [C_{mq} + C_{m\dot{\alpha}}])$ was in most of the comparisons taken to have a fixed value, since the nutations were, except for one case, too poorly defined for amplitude fitting. The value chosen was 5.0. It is this value which together with a K_T of 0.095 gave a good fit to precessional growth rate in the subsonic firings. The absence of noticeable persistent nutations in the computed curves strongly suggests that this value of K_H is too large, and that therefore the K_T is too small. Results for the one round with an extended, clean record of nutations appear to indicate that K_H is quite small between Mach 0.9 and 1.0, but larger below 0.9. There is, however, no indication that K_H is ever negative.

In order to secure good fits in frequency, it was necessary to assume that the main moment coefficient K_M $(\pi/8\ C_{m\alpha})$ was a function of both Mach number and the square of the yaw.

No evident difference was found between the behaviors of the three varieties of the shell tested. Neither machining the rotating band flush with the rear bourrelet nor removing the band entirely seemed to make an appreciable difference in flight behavior, provided always that muzzle velocity and initial spin were held the same.

A consistent peculiarity in the data from the supersonic shots is attributed to a strong wind shear between 9,000 and 11,000 ft. altitude.

THE SONDE

The "yaw sonde" is essentially a miniature radio transmitter which is frequency modulated by a photocell, this photocell being periodically illuminated by the sun shining through a pinhole. The pinhole is in the periphery of the round. The photocell is a circular wafer of silicon mounted parallel to the round's axis and located between the pinhole and axis. The face of the disk is masked except for two narrow strips arranged in a "V" pattern. In flight, once each revolution a small image of the sun, formed by the pinhole, sweeps across the disk, hitting first one arm of the "V", then the other. The position along the lengths of the slits at which it crosses depends on the angle between the axis of the round and a line to the sun.

In the original version of the sonde, the photocell disk was mounted on the axis, and the field of view was about 20°. In order to increase this acceptance angle, so as to permit more flexibility in firing conditions, this Station moved the cell closer to the pinhole, filled the space between pinhole and disk with clear plastic, and added a transistor preamplifier. An acceptance angle of a little more than 90° was obtained, at some sacrifice in resolution. In Fig. 1 are shown the transmitter, which is contained in a fuze body, and the packaged cell and preamplifier. The latter is, in use attached to the inner side of the cylindrical portion of the shell, just under the pinhole. The battery used was a standard fuze type reserve battery, housed in the rear part of the fuze-shaped body.

The radio frequency signal from the sonde is received by a ground station, and the demodulated version recorded on magnetic tape along with timing pulses in I.R.I.G. format B. This demodulated signal consists in a train of pulse pairs, one pair for each revolution. Oscilloscope traces of sections of two such records are shown in Fig. 2, the upper one a good and useful signal, the lower at or below the margin of uselessness. The time between centers of pulse pairs is the reciprocal of the spin frequency, and the ratio of the time between pulses of a pair to that between pairs is a unique measure of the angle sought--that between the round axis and a line to the sun. After each sonde was mounted in the projectile, but before potting, careful measurements were made of the functional relation between this ratio and that angle; and this relationship was later used in reducing the data.

The data on the tape were converted to digital data, also on tape, by NODAC, under human supervision. This new tape in turn was subjected to processing by two successive digital computer programs, the final result being a tabulation of spin rate and orientation angle and its sine against time. Plots of the data, usually even more useful than the tables, were also made.

THE ROUND

All the experimental projectiles used started out as empty standard 5"0 Mk 41 shell. On six of them the rotating band was turned flush with the rear bourrelet, and on four the band was split and entirely removed. Each projectile was then sawn in half, transversely. The front portion was turned internally to a smooth cylindrical surface of length about 3"5, parallel to the axis, and then threaded for 0"75. At about 2"25 forward of the cut, a conical hole (90° full angle) was machined, the axis of the cone being radial with respect to the cylindrical shell body. The intersection of the tip of this cone with the inner machined cylindrical surface formed the pinhole, about 0"050 diameter. Ahead and behind this depression, two countersunk holes were drilled. The

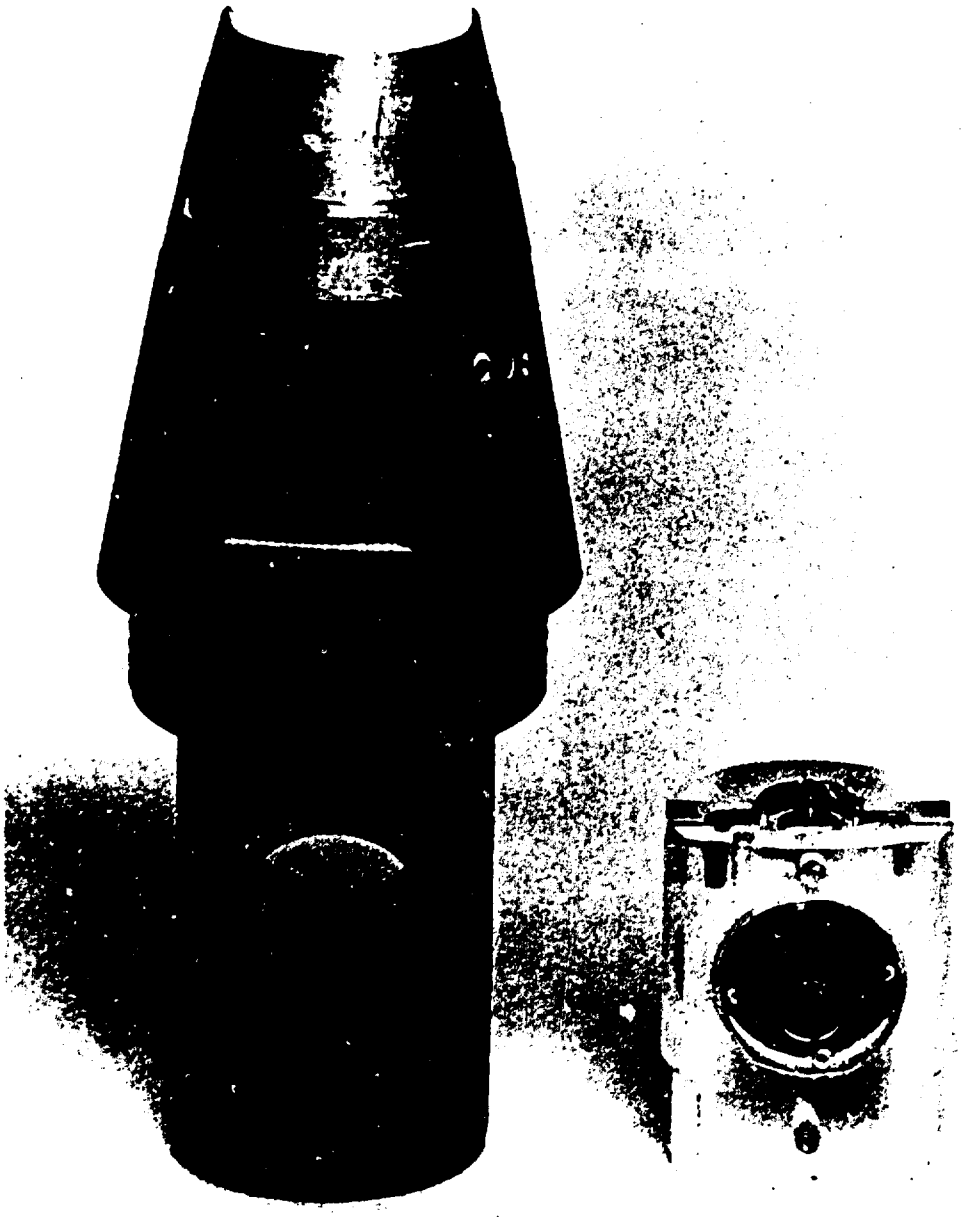

FIG. 1 British Yaw Sonde, With Sensor Modified by Naval Weapons Center.

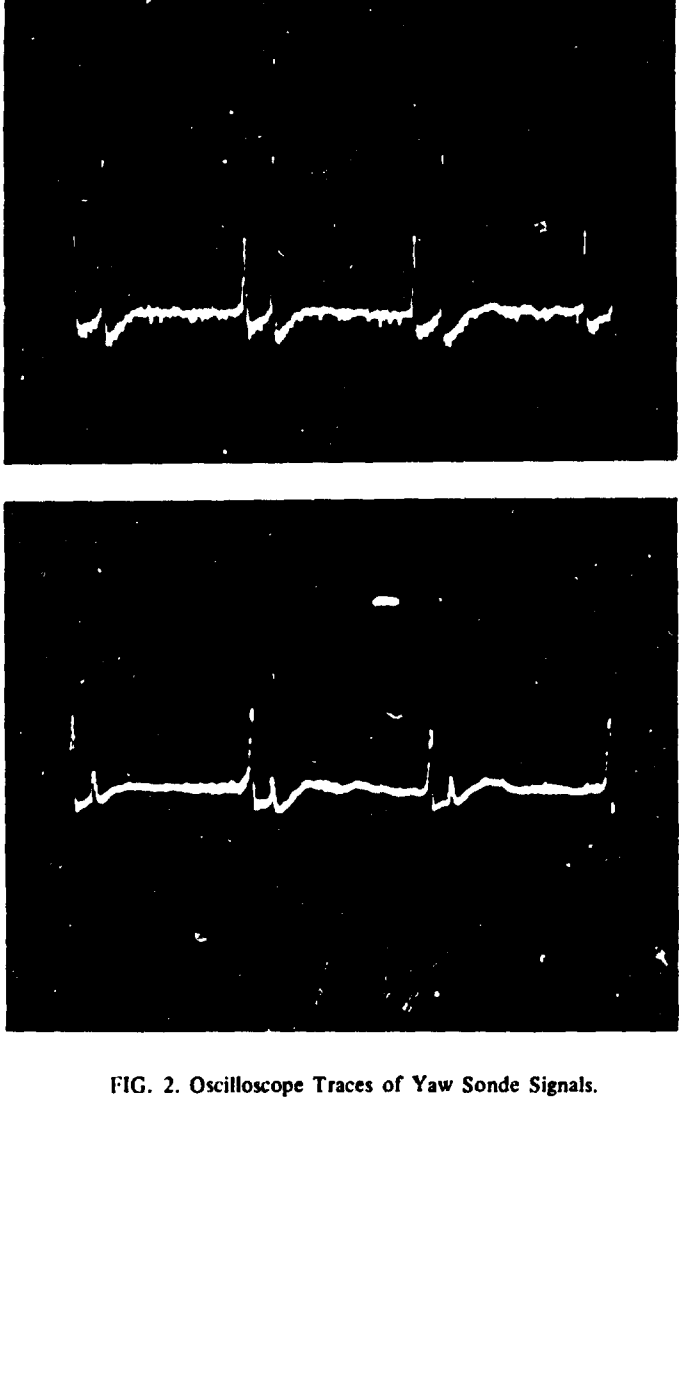

FIG. 2. Oscilloscope Traces of Yaw Sonde Signals.

after part of the projectile was also threaded, from front to back, and an externally threaded sleeve was used to connect the two parts back together (eventually). A non-threaded spacer ring, slipping tightly over the threaded sleeve was used to bring the reassembled projectile back to proper length. Because the sonde transmitter and battery case were housed in a body conforming to the standard NATO artillery fuze (Army M51 family shape), and threads, an adapter was required between the shell body and sonde body. This provided proper threads, length, and contour.

While the shell body was still in two pieces, the assembly of photocell and preamplifier was attached by screws to the interior of the front portion, just under the pinhole. Then the sonde body with transmitter and battery (with adapter) was screwed in and electrical connections made. The sonde was calibrated, using an external source of voltage, a meter, the sun (via a heliostat) as a light source and a dividing head. After the rear and front parts had been reassembled, the interior was filled through the base orifice with an epoxy potting compound, and the base plug inserted. Figure 3 is a photograph of two rounds, one with the standard rotating band and one with none.

It is obvious that the rounds with modified or no rotating band had to be provided with sabots to provide obduration and to impart spin. The sabot designed, Fig. 4, had an aluminum body, a copper skirt, (nearly split), and two steel pins which fitted into holes drilled in the projectile base. This was very successful.

A special experiment was made to determine the powder charges needed to reach the desired muzzle velocities (1240 and 2450 ft/sec) with both standard and saboted rounds. The 2450 ft/sec was chosen deliberately less than service M.V. to ensure safety with saboted rounds.

Table 1 (Appendix A) contains a list of the physical properties of all rounds for which aerodynamic analysis was performed.

RANGE INSTRUMENTATION AND THE FIRINGS

The signals from the yaw sondes were received by two antenna arrays, one vertically, the other horizontally polarized. Each fed a standard automatic frequency-tracking receiver and a pan receiver with scope. The latter permitted rapid location of the signal and lock-on. The demodulated output of each receiver was recorded on tape, both direct and via frequency modulation. IRIG timing signals were recorded on the same tape.

To obtain trajectory and velocity history, the projectiles were tracked with an MSG3A radar, modified to provide improved tracking in range and digital output data.

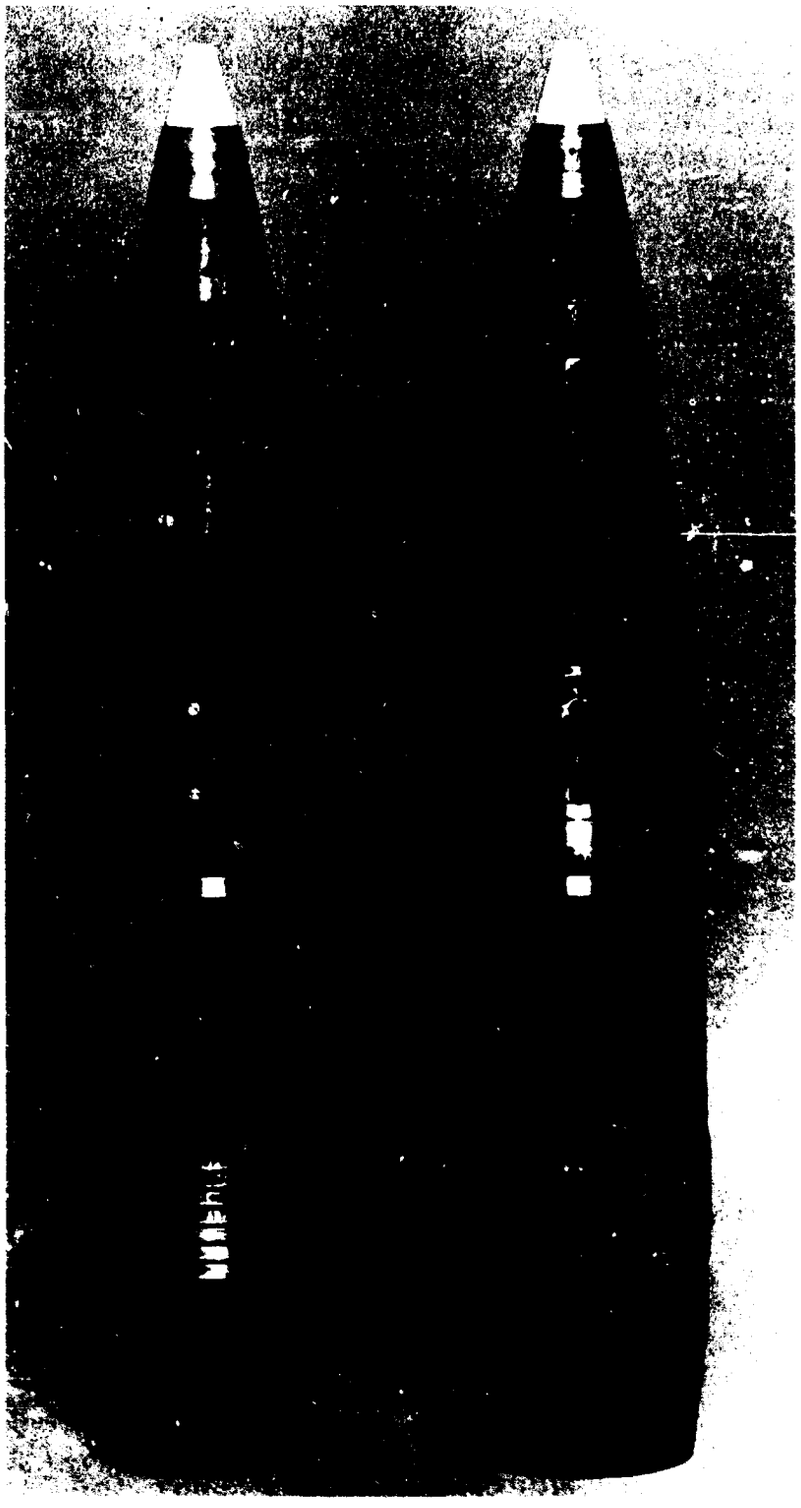

FIG. 3. 5"0 Mk 41 Shell With Yaw Sondes.

FIG. 4. Sabot for 5"0 Mk 41 Shell With Modified or No Rotating Band.

A modified Hawk radar was used in an attempt to get better velocities by the Doppler method. Some good signals were obtained but they always started too late to be of much use.

The initial velocities were measured with sky screens, main reliance being placed on a pair built locally and located at 150 and 200 ft downrange on the gun line. They operated almost perfectly. Backup was provided by a French 2-meter-base sky screen on loan from Aberdeen Proving Ground, and by Bowen cameras. The axes of the sky screens were aligned perpendicular to the gun bore.

Standard meteorological data were obtained, surface temperature pressure and wind being made at about quarter hour intervals during each test, and a balloon ascension to obtain corresponding upper-air data was made shortly before commencement of each day's firings.

Prior to each day's shooting, the time of start and the azimuth of fire were carefully chosen to maximize the time that the sun was in position to be within the receptive cone of a sonde during a whole trajectory.

The first test, E-6293 on 15 December 1966, showed that the methods devised worked, and that one could hope to get good yaw records from half or more of the rounds fired. Radar coverage was marginal. It was hoped to complete the program of firing by the end of calendar year 1967. Crowded schedules, bad weather, and repeated severe difficulties with radar, sky-screens and timing led to delays and a series of abortive tests, so that the shoots weren't completed until 14 May 1968. Difficulties with data reduction and illness of the author delayed the analysis of the data by curve fitting until early 1969.

Table 2 is a list of all rounds for which yaw sonde signals were received, with firing condition. Table 3 lists pertinent meteorological data.

THE THEORY

The equations of motion used in the computation of the curves which were fitted to the data may be divided into two sets. The first set describes a planar particle trajectory and a simple spin history. It also includes an equation for generation of an exponential air density. The second set describes the angular motion of the projectile. It is linearized in that all angles, both of orientation and direction of motion are treated as small deviations from those appropriate to a projectile following with perfect trail a particle trajectory. This still permits nonlinearities to appear in the aerodynamic force system. Also

included in the second set is a calculation of the angle represented by the sonde data. A list of symbols is provided in Nomenclature section.

The force and moment systems used may be described (except for drag) in the body fixed axis system of Ref. 8. The formulas are given here in both aerodynamic and ballistic notation. The first has the advantage of familiarity to a wide circle, but the disadvantage of some ambiguity or lack of agreement concerning sign conventions and use of some factors of 2 in the definition of the derivative coefficients. The second is less known, but is completely unambiguous.

$$F_Y = QSC_{a\alpha}\, v/V = -\rho\, d^2 K_N V v$$

$$F_Z = QSC_{z\alpha}\, w/V = -\rho\, d^2 K_N V w$$

$$M_X = QSd\, C_{\ell p}\, (pd/2V) = -\rho d^4 K_A V p$$

$$M_Y = QSd\, \left[C_{m\alpha}\, (w/V) + C_{np\beta}\, (pd/2V) v/V + (C_{mq} + C_{m\dot{\alpha}})(qd/2V)\right]$$

$$= \rho d^3\, \left[K_M V w - K_T\, pvd - K_H V q d\right]$$

$$M_Z = QSd\, \left[-C_{m\alpha}\, (v/V) + C_{np\beta}\, (pd/2V) w/V + (C_{mq} + C_{m\dot{\alpha}})(rd/2V)\right]$$

$$= \rho\, d^3\, \left[-K_M V v + K_T\, pvd - K_H V r d\right] .$$

The drag force is taken as directed along the relative wind:

$$F_D = QS\, C_D = \rho\, d^2\, V^2\, K_D .$$

This set of definitions implies the following relations:

$$K_D = (\pi/8)\, C_D$$

$$K_N = -(\pi/8)\, C_{z\alpha}$$

$$K_A = -(\pi/16)\, C_{\ell p}$$

$$K_M = (\pi/8)\, C_{m\alpha}$$

$$K_T = -(\pi/16)\, C_{np\beta}$$

$$K_H = -(\pi/16)(C_{mq} + C_{m\dot{\alpha}})$$

In principle all the coefficients are functions of Mach number, V/a, and of the square of the yaw, $|\delta|^2$. In practice only certain ones were so taken:

$$K_M = K_{M0}(\mu) + K_{M\delta 2}(|\delta|^2)$$

$$K_T = [K_{T1}(|\delta|^2)\, f(\mu) + K_{T2}(1-f)]$$

In both of these forms $|\delta|^2$ has its computed instantaneous value. The function $f(\mu)$ was almost arbitrarily taken to be equal to unity for $\mu < 1.0$, to decrease linearly in μ to zero at $\mu = 1.1$, and to stay zero for $\mu > 1.1$.

$$K_D = K_{D0}(\mu) + K_{D\delta 2} \cdot \overline{|\delta|^2}\ .$$

Here $\overline{|\delta|^2}$ is a smooth function of the time, chosen in advance of each particular computation, and intended to represent a sort of average of the running $|\delta|^2$. K_{D0} itself was obtained as $k_1 K_{D00}$, with $K_{D0}(\mu)$ shown graphically in Fig. 5, for which an abbreviated listing is provided as Table 4. K_{D00} is very nearly the drag coefficient of Refs. 2 and 9.

K_{M0} was inserted as $k_2 K_{M00}(\mu)$ where K_{M00} is as follows:

	K_{M00}
$\mu < 0.755$	1.621
$0.735 < \mu < 0.910$	increases linearly to 1.937
$0.910 < \mu < 0.96$	decreases linearly to 1.752
$0.96 < \mu < 1.10$	constant at 1.752
$\rho > 1.10$	constant at 1.752 for subsonic shots; decreases linearly for supersonic shots, being 1.522 at $\mu = 2.00$.

This form was chosen as a result of several preliminary fitting attempts.

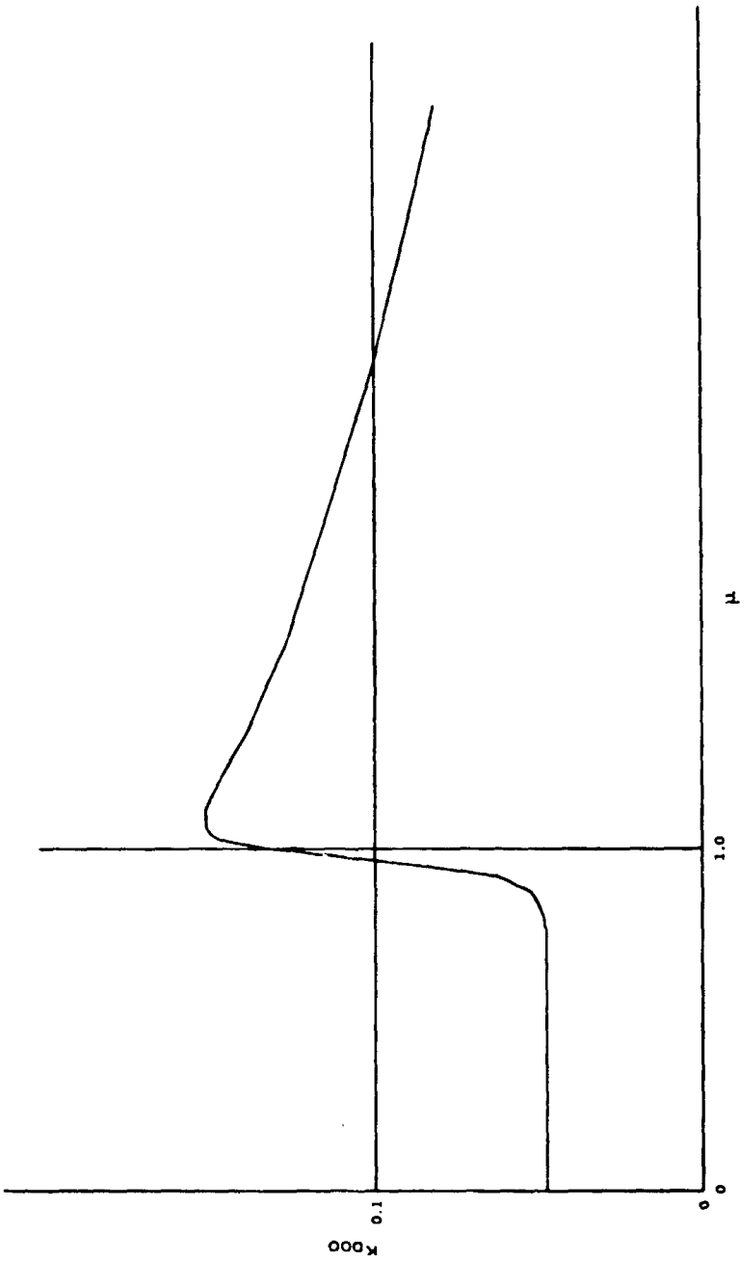

FIG. 5. Drag Coefficient of 5"/0 Mk 41 Shell.

For convenience, certain auxiliary quantities are defined:

$$U = V/d$$

$$\nu = 2\pi n/\nu$$

$$D = \rho d^3 K_D/m$$

$$N = \rho d^3 K_N/m$$

$$L = N - D$$

$$A = \rho d^5 K_A / I_p$$

$$M = \rho d^5 K_M / I_T$$

$$H = \rho d^5 K_H / I_T$$

$$T = \rho d^5 K_T / I_p$$

$$G_1 = g \sin \alpha / d U^2$$

$$G_2 = g \cos \alpha / d U^2 .$$

The independent variable corresponding to machine time was chosen to be s, the dimensionless arc length. This variable never appears explicitly in the equations, serving only as a variable of integration. Its time derivative is U.

The first set of equations is

$$t' = 1/U \tag{1}$$

$$U' = - DU - g \sin \alpha/Ud \tag{2}$$

$$\alpha' = - G_2 = - g \cos \alpha/d U^2 \tag{3}$$

$$n' = - An \tag{4}$$

$$\rho' = - \gamma d \rho \tag{5}$$

$$x' = d \cos \alpha \tag{6}$$

$$y' = d \sin \alpha \tag{7}$$

The second set of equations is

$$\delta = \phi - \theta \tag{8}$$

$$\theta = L\,\delta + G_1\,\theta \tag{9}$$

$$\phi'' = [i\nu - (H - D - G_1)]\,\phi' + (M - i\nu T)\,\delta + i\nu G_2 \tag{10}$$

$$\sin \sigma = [(\cos \alpha - \phi_2 \sin \alpha) \cos A_S + \phi_3 \sin A_S] \cos E_S + (\sin \alpha + \phi_2 \cos \alpha) \sin E_S \tag{11}$$

Equations 8, 9, and 10 each represent, of course, two real equations. Note that "sin σ" is really the cosine of the angle between the projectile axis and a line to the sun.

Note that no provision was made to take account of wind.

The equations were realized on an Electronics Associated computer. Almost all components available from one console and about half those of another were used.

K_{T2} was taken as constant, approximately -.024. $K_{TL}(|\delta|^2)$ was set in as a series of three or four segments each linear in $|\delta|^2$. The general form chosen was based on previous experience with other projectiles, and proved to be quite adequate in this case.

CURVE FITTING

Samples of the data and fits to them are shown in Appendix B, Plates IA-VIE. For example, Plate IA is a plot of velocity, trajectory and spin data for Round 11 of E-6293, and the overlay IB shows the corresponding computed curve. Plate IC is the yaw sonde record, as $\sin \sigma$, while the overlay ID contains the computed version, as well as $|\delta|^2$, $\rho_o T\,(|\delta|^2)/\rho$ and $K_{M00}(\mu)$. Taking the vertical distance between $\sigma = 0.0$ and $\sigma = 1.0$ as unity for the other curves also, the plots represent $100\,|\delta|^2$ in radians squared, $1.2 \cdot 10^{-3} T$, and $0.457\,K_{M00}$. In this particular case $\rho_o T/\rho$ is $5 \cdot 10^{-3}$ for δ^2 small, and is zero at $\delta^2 = 50.0 \cdot 10^{-4}$ rad^2.

The smooth curve approximating $|\delta|^2$ is the $|\delta|^2(t)$ that was used in this case. The other sets of plates correspond, in general, to the same pattern.

Fitting for the subsonic shots proceeded as follows. A plot of V, y, x and n versus time was placed on the table and overlaid with vellum. The physical parameters of the round, surface air density, velocity of sound, and guessed values of the aerodynamic coefficient functions were inserted (as k_1, k_2, T (δ^2), N, etc.) by potentiometer settings, as were also initial conditions U_o, α_o, n_o, and computed curves of the four dependent variables drawn by the plotter, driven by the computer. By successive trials of different k_1 (drag) values and of slight changes in α_o and occasionally U_o, the fits between computed and measured curves of V and y were improved. Then the n fit was improved by adjusting K_A.

The second step (after setting in sun azimuth and elevation) was to place a plot of the measured sin σ vs. t curve on the plot table, overlay it with vellum, guess initial ϕ_2 ϕ_3, ϕ_2' and ϕ_3', (θ_2 and θ_3 were taken always as zero initially), and have the machine superimpose its computed sin σ curve on the data. Then the sun angles, A_S and E_S were adjusted by small amounts and by trial and error until the general trends of the two sin σ curves were in fair agreement. This adjustment was usually 1 to 3 degrees, but in two cases, that to E_S was much larger, and in one case that to A_S. Following this, adjustments were made to the $T(\delta^2)$ function, and occasionally to k_2 (affecting K_M). Emphasis at this stage was on ensuring that there were no major discrepancies in the computed yawing frequencies, and that the initial amplitude, rate of growth and final steady amplitude of the precessions were nearly right.

Since it had been found in early trials that good fits to both the V and y curves could not be obtained without allowing some effect of the yaw on drag, the computed δ^2 was plotted, and a function unit set up to provide a smooth function of time nearly reproducing a running mean of δ^2. Attention was then returned to the plot of trajectory variables. k_1 and α_o were readjusted, now along with the parameter $K_{D\delta 2}$, until satisfactory matches in V and y were obtained simultaneously. (When this had succeeded, the x curves were also satisfactory.) Any necessary readjustment of K_A was then made.

Finally a definitive fit to the sin σ curve was made, again by trial-and-error. This time $K_{m\delta 2}$ was varied, as well as k_2 and $T(\delta^2)$, and the initial conditions. Here an attempt was made not only to reproduce the amplitude behavior of the precessions but also their phase. We tried to obtain good fits to phase and frequency both on the very early and very late oscillations and a good average frequency in the middle. No phase errors over about 1/4 cycle are evident in the final fits.

Control of Magnus moment was exercised through the function

$$T_o(\delta^2) = \rho_o T/\rho = \rho_o d^5 K_T / I_p .$$

For most fits this was a constant from $\delta^2 = 0$ to $\delta^2 = \delta_1^2$, typically $40.0 \cdot 10^{-4}$ rad^2, then decreasing linearly to some negative value at $\delta^2 = \delta_2^2$, becoming zero at $\delta^2 = \delta_1^2 + 10.0 \cdot 10^{-4}$, and being a negative constant for $\delta^2 \geq \delta_2^2$. In a few cases this functional behavior was replaced by one breaking more gently, i.e., positive $T_o = T_{oo} > 0$ for $\delta^2 \cdot 10^4 < 37.0$, decreasing linearly to $0.80\, T_{oo}$ at $\delta^2 \cdot 10^4 = 42.0$, then linearly to a negative value at δ_2^2, being zero at $\delta^2 \cdot 10^4 = 50.0$, and a negative constant for $\delta^2 \geq \delta_2^2$. The substitution of this function for the previous one (for the $\delta_1^2 \cdot 10^4 = 40.0$) made no change which could be detected in the yawing motion. Broadening the transition further, by making the decrease from T_{oo} to zero take place linearly over a δ_1^2 range of $20 \cdot 10^{-4}$ was less satisfactory. Increasing the steepness of the transition helped the behavior of nutation amplitude slightly, but could not be tolerated during much of the time for it caused erratic computation. Most of this erratic behavior was eventually traced to a particularly touchy electronic multiplier, but too late for new trials to be attempted. For all rounds but numbers 5 and 7 of E-7274, 3 April 1968, it was satisfactory to place the zero of T at $\delta^2 = 50.0 \cdot 10^{-4}$ rad^2. For the exceptional two rounds it was necessary to shift the whole $T(\delta^2)$ curve bodily along the δ^2 axis.

In a few cases the early nutations were clear enough so that it was worth attempting to fit their phase and frequency. This was tried using plots with an enlarged time scale. Small adjustments of 1% or less were needed to the nominal ratio I_p/I_t, and corresponding changes in $k_2(K_M)$ to secure fit of both nutation and precession frequencies. These adjustments are well within the precision of measurement of that ratio. The fit so obtained was the best one for the first few seconds. On returning to the plot for the whole flight, using the new I_p/I_t, a further small adjustment of K_M was needed to get the best phase behavior averaged over the whole trajectory. In one case the nutations were clear enough so that comparison of computed with measured amplitudes was meaningful. In this case it was not possible to fit these amplitudes and the precession behavior using a constant K_H. In fact, in order to get the nutations to persist long enough for a 10-second fit in phase, a combination

of K_H and K_T had to be used which was grossly wrong when the behavior in the large was considered. Implications are discussed in a later section.

K_N was taken as the constant 0.80 for all rounds. It was intended that K_H would be 5.00 for all rounds. By inadvertence some of the actual values deviated a little from this, but by amounts which (as shown by actual test in the worst case) did not visibly affect the plots.

The data from the supersonic rounds were fitted in the same way, except for the four following changes:

1. K_D was not made to depend on $\overline{|\delta^2|}$. Instead, a constant was added to $k_1 K_{D0}$.

2. The function $K_M(\mu)$ was different for $\mu > 1.10$. (This change would not have affected the subsonic fits except to require slightly different initial conditions, for on none of these was $\mu > 1.1$ where there were sonde data.)

3. To obtain the late precessions in anything like the measured amplitude, and without using combinations of H and T which were very different from those giving fits to the subsonic data, it was necessary to simulate small disturbances to the projectile on the downward leg of the trajectory. A small kick at about 50.0 sec was imparted (mathematically) to the round.

4. At about 62 sec flight time all supersonic rounds, even those for which fits were not attempted, for one reason or another, showed a decrease of a few degrees in the smoothed level (not amplitude) of σ, taking place over one or two precession periods. This could not in any way be fitted by our model, and no attempt was made.

THE INDIVIDUAL ROUNDS

Plates IA through VIE of Appendix B show computer fits to both trajectory elements and yawing motion for rounds as follows: Rd. 11 of E-6293, Rds. 5, 7, 8 and 10 of E-7274A (3 Apr 1968) and Rd. 8 of E-7274B (14 May 1968). For each set of plates the Roman numeral indicates the round. The plate with the A designator is a plot of the measured trajectory elements, and the B overlay shows the computed elements. Those designated C (and VE) are xerographic copies of the yaw sonde data as plotted by the 1108 computer and 4060 plotter, while those designated D (and VF and VIE) show the computed fit to that data and some auxiliary curves. Note that the time scales of Plates IC through VC have an

arbitrary origin. True zero time is indicated by the left hand vertical dashed line. Time origin is correct in VIC. Note also that the sign of (sin σ) has been reversed in plotting.

The aerodynamic parameters used in obtaining the computed curves are listed in Table 5 for the six rounds illustrated and for the four additional ones which were analyzed in detail.

Comments follow on each round for which any yawing data was obtained.

SUBSONIC SHOTS

E-6293, Rd. 10: Standard Band. Yawing record obtained from 1 to 2 and 4 to 33 seconds. Somewhat noisy. Almost no change was found in the computed curve of sin σ on going from the sharp shouldered to rounded shouldered curve of $K_T(\delta^2)$, though the δ^2 curve showed slightly larger, (but still very small) persistent nutations. From 13 to 23 seconds the nutations were almost good enough to fit for phase. A plausible fit to frequencies of both nutetion and precession was obtained by lowering the ratio I_p / I_T by 2% from that from Table 1, and K_M by 1% from the value in Table 5. Note, however, that I_p and I_T were not actually known for this round (nor Rd. 11). The values of Table 1 are means for the lot. Steady precession of about 4°.

E-6293, Rd. 11: Standard Band. Yaw record from 1 to 33 sec. Nutations seem smaller than usual. This record was noisy and was subjected to filtering before plotting, which may have attenuated the nutation amplitude, though the filter was designed to avoid this. Steady precession of about 4°. See Plate Set I.

E-7274A, Rd. 4: Standard Band: Yaw record from 2 to 34 sec. From 4 to 24 sec. the amplitude of the precession is steady at about 4°. Then over about 3 sec, it decreases to about half size and stays so till impact. Little, if any, nutations visible except initially.

E-7274A, Rd. 5: Standard Band: Yaw record noisy, 2 to 6 sec, then good to 34 sec. Persistent small nutations visible. Precession amplitude large, about 5° from 10 to 21 sec, then decreasing as in Rd. 4, to about 3°½. See Plate Set II.

E-7274A, Rd. 7: Flush Band. Yaw record from 7 to 33 sec. Nutations visible but unreliable for phase fitting. Steady precession amplitude smaller than usual, about 2°8. See Plate Set III.

E-7274A, Rd. 8: Flush Band. Yaw record from 0.5 to 33 sec. Note that no trajectory data were available for this round. It was analyzed

because it was the only nearly complete yaw record for a projectile of its type and speed, and because of the unexpectedly small precession of Rd. 7. In obtaining the fit to the sonde data, the trajectory data were assumed to be the same as for Rd. 7. Note that the bursts of nutations seen in the computed δ^2 curve between nominal times of 6 to 8, 11 to 28, and 32 to 34 seconds are machine artifacts. In early fitting trials for this round it was found that the growth rate of the precessions was unaffected by concurrent variations of K_H and K_T so long as the following approximate relation was obeyed: $0.16\ H_o + T_o = \text{constant}$. Here the subscripts indicate subsonic, zero yaw, standard air density values. See Plate Set IV.

E-7274A, Rd. 9: Flush Band. Similar to Rd. 8. No trajectory available. Sonde record shorter than for Rd. 8.

E-7274A, Rd. 10: No Band. Yaw record from 3 to 33 sec. Nutations present, and clear from 3 to 19 sec. To fit both frequencies between 3 and 13 sec, I_p/I_T had to be reduced by 0.6% from that deduced from Table 1, and K_M by 1.5% from that of Table 2. In order to keep the computed nutations large enough long enough, the drastic measure was taken of raising $K_{T1}(0)$ to .1568 and dropping K_H to 1.41. This pair gave unacceptable growth of the nutation for $t > 13$ sec, but still allowed the nutations to decay too rapidly between 3 and 6 sec. On reinstating the original (Table 5) values of $K_T(0)$ (0.0941) and $K_H(5.00)$, but keeping the new value of I_p/I_T, a good fit to precession phase over the whole record was secured, with a K_M only slightly larger. With the original values of I_p/I_T and K_M, it was found that precession growth was unaffected by joint change of K_T and K_H so long as $.174\ H_o + T_o = \text{constant}$. See Plate Set V.

E-7274A, Rd. 11: No Band. Yaw record 13 to 33 sec. Some indication of precessions 8 to 13 sec, but in bad noise. Nutations good from 20 to 30 sec. Fit to both frequencies required decreasing I_p/I_T by 1.2% and K_M by 1.4%. These new values also gave a good fit over the whole record. Computed nutation amplitude was maintained nearly steady as in the actual data, over the interval 20 to 30 sec by using $K_T(0)$ of .1516 and a K_H of 1.43, but this set of values again gave unacceptable nutation growth for $t > 30$ sec.

SUPERSONIC SHOTS

Unfortunately, no good yawing records of unmodified (standard band) projectiles were obtained in this series of experiments. On the other hand, one good record for the standard round was obtained on 8 November 1965, during test E-5415, which was conducted in connection with RAP development. This record for that test's Round 6, extends from 15 to 80 sec time of flight. It is smooth, with no visible oscillations until about 65 sec, when a small precession appears, then slowly grows, attaining an amplitude of about 2° or a little more by impact. In 1965 the available radars were unable to provide data smooth enough so that good velocity data could be derived.

E-6293, Rd. 5: Standard Band. Yaw record almost useless because of noise, but it contains a suggestion of precession just before impact.

E-6293, Rd. 7: Standard Band. Yaw record stops at 40 sec.

E-7247B, Rd. 5: Standard Band. Yaw record very noisy. Precession visible from 57 sec. A shift in average level of $\sin\sigma$ occurs at 63 sec without noticeably changing the precessional amplitude. (This type behavior was found for all rounds of E-7274B.)

E-7274B, Rd. 7: Flush Band. Yaw record from 4 to 76 sec. Similar to Rd. 8. Precession becomes visible about 53 sec. Shift at 64 sec. Less trajectory data than for Rd. 8.

E-7274B, Rd. 8: Flush Band. Yaw record from 5 to 76 sec. Precession visible from 51 sec. Shift at 64 sec. The $K_T(0)$ value of Table 5 (.1393) gave the fit of Plate VID when the round was given a small kick at t = 47.5 sec. The fit of Plate VIE was obtained by eliminating the kick, but increasing $K_T(0)$ to 0.1857. $K_T(0)$ of 0.0928 used with a double-sized kick gave an amplitude of about the right eventual size but too slow a growth. See Plate Set VI.

E-7274B, Rd. 10: No Band. Yaw record from 15 to 73 sec. Precession visible from 52 sec. Shift at 61 sec. Amplitude at 73 sec about 3°. Got fit with $K_T(0)$ of 0.1352 and a small kick at t = 53.0 sec. Also got a good fit with same K_T without kick but with large initial yaw.

E-7274B, Rd. 11: No Band. Yaw record from 16 to 76 sec. Similar to Rd. 10. Precession visible from 49 sec. Shift at 62 sec. Amplitude at 76 sec, a little less than 4°.

DISCUSSION

The drag values deduced from the trajectory fits must not be taken too seriously, especially the very low scale factors k_1 and the large flat corrections found for the two supersonic shots. In the first place, the velocity determinations are among the most imprecise of the data obtained. In the second place, no attempt was made to get the best possible drag values. So long as fits $V(t)$ and $y(t)$, good enough to serve as a basis for calculating the angular motion, were obtained, no more was required. In the third place, no allowance was made for wind. This neglect was probably particularly influential in affecting the deduced values of drag for the supersonic shots, for in those cases there was a large head wind at altitudes above 9,000 ft, and it is primarily, though not only, the velocity behavior at high altitude that required the large flat correction, compensated on the upward trajectory leg by a low k_1.

The facts that in seven cases the sun had to be "moved" slightly, and that even so, the general trends of the $\sin \sigma$ curves are not perfect over the whole flights are probably due to two causes: slight errors in sonde calibration and neglect of wind.

Both Rounds 4 and 5 of E-7274A showed two levels of steady precession amplitude, but the exactly similar Rounds 10 and 11 of E-6293 did not. In addition, the earlier level of Round 5, E-7274A was unusually large. Round 7 of E-7274A did not show the shift of amplitude, but did have an unusually small precession, contrary to what was found for the similar Rounds 8 and 9 of the same day's test. These discrepancies may represent real effects. Still queerer Magnus behavior has been found for some rockets. But it should be noted that it is in just these three cases that the largest adjustments to the sun angles were needed. For Round 4 the sun azimuth had to be adjusted by 6°. For Round 5 the sun elevation was changed by 11° and for Round 7 by 6°. It is considered most likely that these peculiarities are all due to shifts of the sonde components between calibration and flight.

All the rounds of E-7274B (supersonic shots) showed a peculiar shift of the level of $\sin \sigma$ about which oscillations were occurring. This shift took place at a little over 60 seconds time of flight, when the projectiles reached about 11,000 ft altitude on the descending leg of the trajectory. Now there was a strong wind shear between the altitudes of 9,000 and 12,000 ft, the speed changing from 27 ft/sec at the lower altitude to 92 at the higher, and the direction changed by nearly 90 deg. Furthermore, the shift was not observed on Round 6 of E-5415. It is believed that the shift was caused by the wind shear. This belief was tested by placing the problem on a digital computer. The exact six-degree-of-freedom equations were used and the parameters supplied for

Round 10 of E-7274B. Two runs were made, one with and one without the measured wind. The latter portion of the "sin σ" plot for the case with wind is shown in Plate VII. One can see the shift of mean value taking place at about 64 sec. (Remember that there is an artificial reversal of sign between the earlier plates and this one.) No such shift was found in the curve computed with no wind.

The values of K_A, the spin damping coefficient, scatter a good deal. In particular, there is no explanation of why larger values were needed for the two rounds of E-6293 than for Rounds 4 and 5 of E-7274A. Comparison among the six values for E-7274A suggests that the value of K_A may really be smaller for the rounds with flush rotating bands than for those with either the standard, engraved band, or no band at all. The bottom of the band groove of the latter preserved the knurling.

It appears certain that from the Mach number of 0.70 to at least one of 0.95 the Magnus moment coefficient changes sign extremely rapidly near a yaw angle of about 4^{o}, for all three versions of the projectile. In fact, the data do not exclude an actual discontinuity in the Magnus moment. The level and functional form of the coefficient at larger angles was not determinable from the data. Neither could the data determine the Magnus moment at supersonic speeds, but no disagreement was found with the conclusion from spark range experiments that supersonically K_T has a small negative value.

The values in Table 5 of $K_{T1}(0)$, the value of K_T at very small yaw angles and subsonic speeds must not be considered as definitive. In the first place, they were determined by considering only the behavior of the precessions, and then under the assumption that K_H was 5.0. Without taking into account the behavior of nutation amplitude, neither K_T nor K_H can be determined separately. Besides there is no reason to believe that the functional dependence of either coefficient on Mach number and yaw is as simple as assumed. But some simple choice of form had to be made. With each additional complexity admitted, the amount and quality of the data needed to fix parameter values, and the uncertainty of the latter, increase. The data on precessional growth, for the two rounds (8 and 10 of E-7274A) for which this is most completely visible, required that very nearly $K_T / A + K_H / 6B$ = constant. Quick trials on two other rounds showed that this relation gave good results there also. Now the factor 1/6 corresponds to a stability factor of about 1.8, and to a ratio of nutation to precession frequency of about 5. These are both values appropriate to the conditions during the early growth of the precessions. The ratio of frequencies was confirmed by actual counting. Note that for the rounds fired supersonically the flight conditions during the time they show noticeable precessions were such that the factor 1/6 should be replaced with one nearer 1/20. Now most, but not all, of the subsonic shots showed small persistent nutations superimposed on the much larger steady precession. This is

not reproducible with the listed parameters. On the other hand, the nutation fitting done on Rounds 10 and 11, especially the latter, where the Mach number range involved was 0.73 to 0.79, indicates that a $K_{T1}(0)$ of 0.157, with a corresponding K_H, is too large. The behavior of the two supersonic shots led to a choice of $K_{T1}(0)$ of greater than 0.13, with $K_H = 5.0$. It is, therefore, believed that very good estimates for $K_{T1}(0)$ and K_H are 0.14 and 1.8, respectively, for $0.7 \leq \mu \leq 0.9$. In the case of Round 10, E-7274A, the nutations were even more slowly damped initially, that is for $0.9 < \mu < 1.0$, than would be computed from these estimated coefficients. But the precessions are growing. It is therefore likely that over the latter range of Mach number K_H is even smaller. It may even be negative over a small interval, though there is no proof of this. The negative values of K_H deduced from some spark range shots are of uncertain significance, for they result from an entirely linear analysis, and are, at best, badly scattered.

In conclusion, the 5"0/54 shell, Mk 41, develops a definite limit cycle in precession, of amplitude about 4^o when flying at speeds between Mach numbers of 0.7 and 1.0. This shows up drastically on low velocity shots, and more gently, in the case of shots fired at high velocity, in the development of decided, though probably harmless precessions on the downward legs of long trajectories. This behavior is undoubtedly due to the large and very nonlinear Magnus moment at subsonic speeds.

Appendix A

TABLES

TABLE 1. Physical Properties of Rounds

Average length overall 26.10 in.

E. No.	Rd. No.	m, lb	c.g. (in fr. tail)	I_p lb in^2	I_T lb in^2	Type
6293	10	68.10	-	240.9	2619	Std
	11					Std
7274A	4	67.95	9.34	240.9	2549	Std
	5	68.71	9.39	240.2	2669	Std
	7	67.58	9.43	240.2	2608	Fl B
	8	67.95	9.49	241.8	2644	Fl B
	10	66.91	9.56	235.5	2651	No B
	11	66.97	9.58	234.3	2619	No B
7274B	8	67.95	9.50	241.8	2645	Fl B
	10	67.00	9.58	234.7	2629	No B

TABLE 2. Firing Conditions

Test No.	Date	Rd. No.	Type	Time[a]	Q.E.	MV ft/sec[b]	Sonde Record	Radar Coverage
E-6293	15 Dec 66	5	Std	1426	30°	2466	poor	good
		7	Std	1445	30°	2561	short	good
		10	Std	1530	30°	1230	good	good
		11	Std	1536	30°	1242	good	good
E-7274A	3 Apr 68	4	Std	1455	30°	1227	good	good
		5	Std	1504	30°	1231	good	good
		7	Fl Bd	1521	30°	1167	short	good
		8	Fl Bd	1545	30°	1187	good	none
		9	Fl Bd	1555	30°	1180	fair	none
		10	No Bd	1607	30°	1200	good	late
		11	No Bd	1614	30°	1200	good	late
E-7274B	14 May 68	5	Std	0732	45°	2416	poor	good
		6	Std	0747	45°	2360?	poor	useless
		7	Fl Bd	0801	45°	2456	good	fair
		8	Fl Bd	0814	45°	2458	good	good
		10	No Bd	0832	45°	2474	good	good
		11	No Bd	0846	45°	2434	good	short

[a] Times for E-6293 and E-7274A are PST; for E-7274B they are PDT.

[b] The MV values are instrumental and are not corrected back to emergence.

TABLE 3. Meteorological Data

h,ft,MSL	6293		7274A		7274B	
	$\rho \cdot 10^3$, slug/ft^3	T deg C	$\rho \cdot 10^3$, slug/ft^3	T deg C	$\rho \cdot 10^3$, slug/ft^3	T deg C
2185	2.20	16.6	2.14	22.1	2.24	9.7
3000	2.17	13.7	2.11	17.3	2.18	8.9
4000	2.10	11.3	2.06	14.4	2.11	7.2
5000	2.04	9.8	2.00	11.5	2.05	5.0
6000	1.97	8.2	1.96	8.6	1.99	2.8
7000	1.91	6.8	1.90	5.6	1.94	0.1
8000	1.85	5.3	1.85	2.6	1.88	-2.8
10000					1.78	-8.0
15000					1.47	-9.4
20000					1.25	-19.5
25000					1.06	-29.4
30000					0.90	-42.0
Winds	< 3 ft/sec, surface < 27 ft/sec to 8000 ft		< 22 ft/sec, surface < 16.8 ft/sec to 8000 ft		< 7 ft/sec, surface increasing to 33 at 11,500 ft and to 90 at 14,000 ft	
Used ρ, Surface Temp	$2.21 \cdot 10^{-3}$		$2.15 \cdot 10^{-3}$		$2.24 \cdot 10^{-3}$	
	16°.0 C		14°.5 C		0°. C	
a	1119 ft sec		1116 ft sec		1087.6 ft sec	
γ	$.306 \cdot 10^{-4}$ per ft		$.258 \cdot 10^{-4}$ per ft		$.316 \cdot 10^{-4}$ per ft	

TABLE 4. Drag Function

Mach No.	K_{D0}	Mach No.	K_{D0}
0.0	0.0475	1.3	0.1448
0.7	0.0475	1.4	0.1390
0.8	0.0480	1.6	0.1302
0.9	0.0558	2.0	0.1170
1.0	0.1261	2.2	0.1105
1.1	0.1539	2.4	0.1041
1.2	0.1488		

TABLE 5. Aerodynamic Parameters of Successful Fits

K_N uniformly 0.800.

E No.	Rd No.	K_A	K_1	$K_{DO}(.7)$	$K_{D\delta}2$ [a]	ΔK_D [b]	K_H	k_2	$K_M(.7)$	$K_{M\delta}2$ [a]	ΔK_M [b]	$K_{T1}(0)$ [c]	$\delta_o^2 \cdot 10^4$ [d]	Type
6293	10	0.00626	0.993	0.0472	7.17	0.0323	5.00	1.013	1.641	0	0	0.0937	50	Std
	11	0.00685	1.104	0.0524	4.42	0.0199	5.00	1.033	1.675	-11.28	-0.051	0.0937	50	Std
7274A	4	0.00529	0.962	0.0457	4.53	0.0204	4.87	1.097	1.697	-19.81	-0.089	0.0963	50	Std
	5	0.00529	0.973	0.0462	4.58	0.0706	5.00	0.995	1.612	- 2.96	-0.013	0.0960	75	Std
	7	0.00427	1.041	0.0495	0	0	4.89	1.005	1.629	-14.48	-0.065	0.0960	25	Fl Bd
	8	0.00430	1.041	0.0495	0	0	4.95	1.019	1.651	-23.49	-0.105	0.0967	50	Fl Bd
	10	0.00580	1.226	0.0582	2.23	0.0100	5.00	0.995	1.612	-17.66	-0.079	0.0941	50	No Bd
	11	0.00546	1.227	0.0583	2.23	0.0100	5.14	0.996	1.614	-17.45	-0.079	0.0937	50	No Bd
7274B	8	0.00464	0.703	0.0334	—	0.0326	5.00	1.005	1.629	-14.11	-0.063	0.1393	50	Fl Bd
	10	0.00563	0.804	0.0382	—	0.0322	5.00	1.089	1.764	0	0	0.1352	50	No Bd

[a] $K_{D\delta}2$ and $K_{M\delta}2$ are in $(\text{rad.})^{-2}$.

[b] ΔK_D and ΔK_M are given for $\delta^2 = 45.0$ rad.^{2} for subsonic shots.

ΔK_D for supersonic shots is a flat correction to $K_1 K_{DOO}$.

[c] $K_{T1}(0)$ is the subsonic value of K_T at $\delta^2 = 0$ used with the listed K_H to obtain a fit.

For subsonic shots (E-6293 and E-7274A) it corresponds to $1.2 \cdot 10^5 P_o T/\rho = 6.00$.

For the supersonic shots to $1.2 \cdot 10^5 P_o T/\rho = 9.00$.

[d] δ_o^2 is the yaw squared in rad^2 at which the subsonic K_T was zero. Supersonic K_T always $\simeq -0.024$.

Appendix B

PLATES

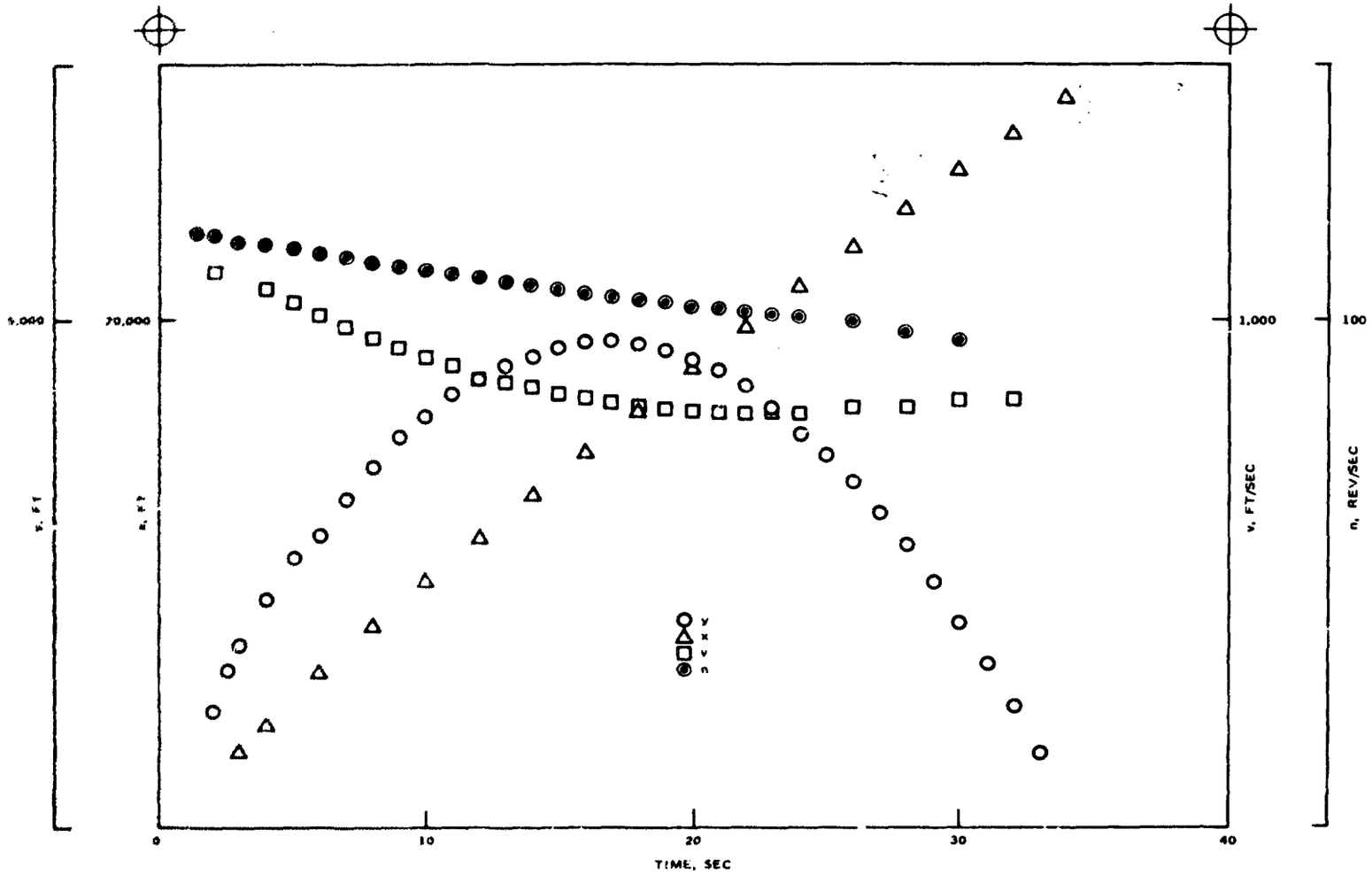

A.

PLATE I. E-6293, Round 11.
A. Trajectory data.
B. Computed trajectory elements.

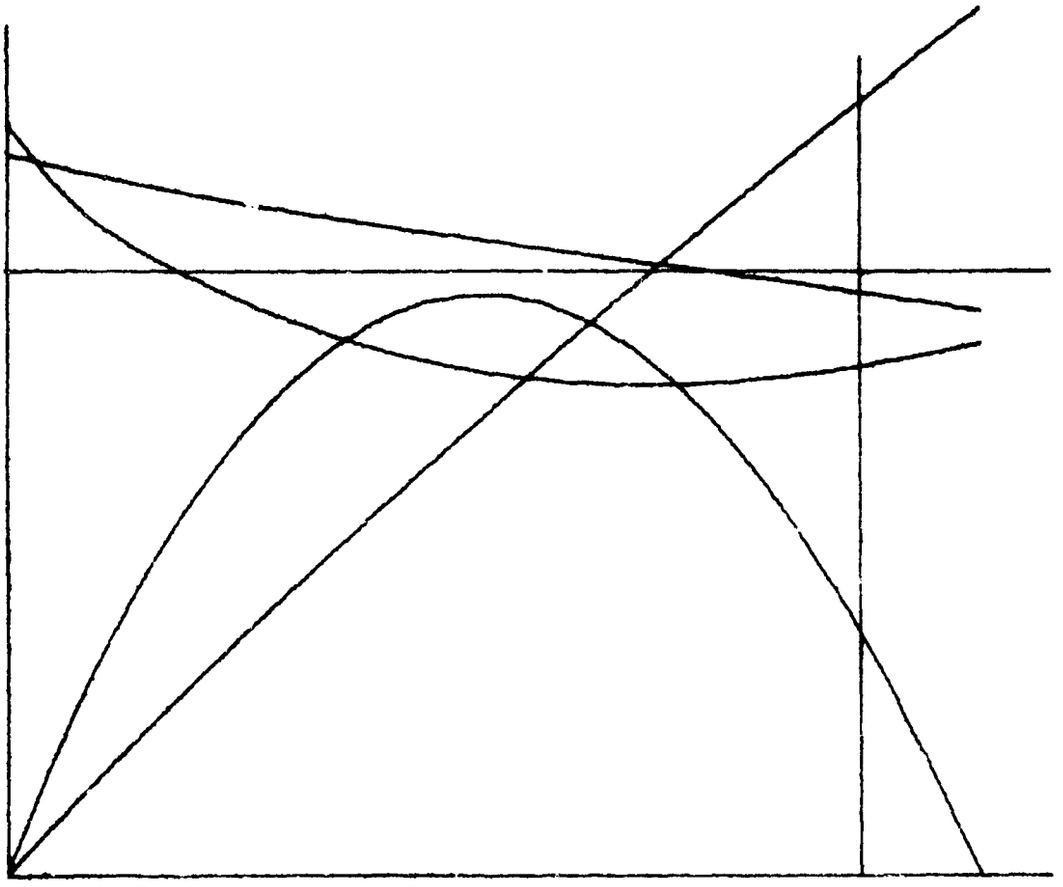

B.

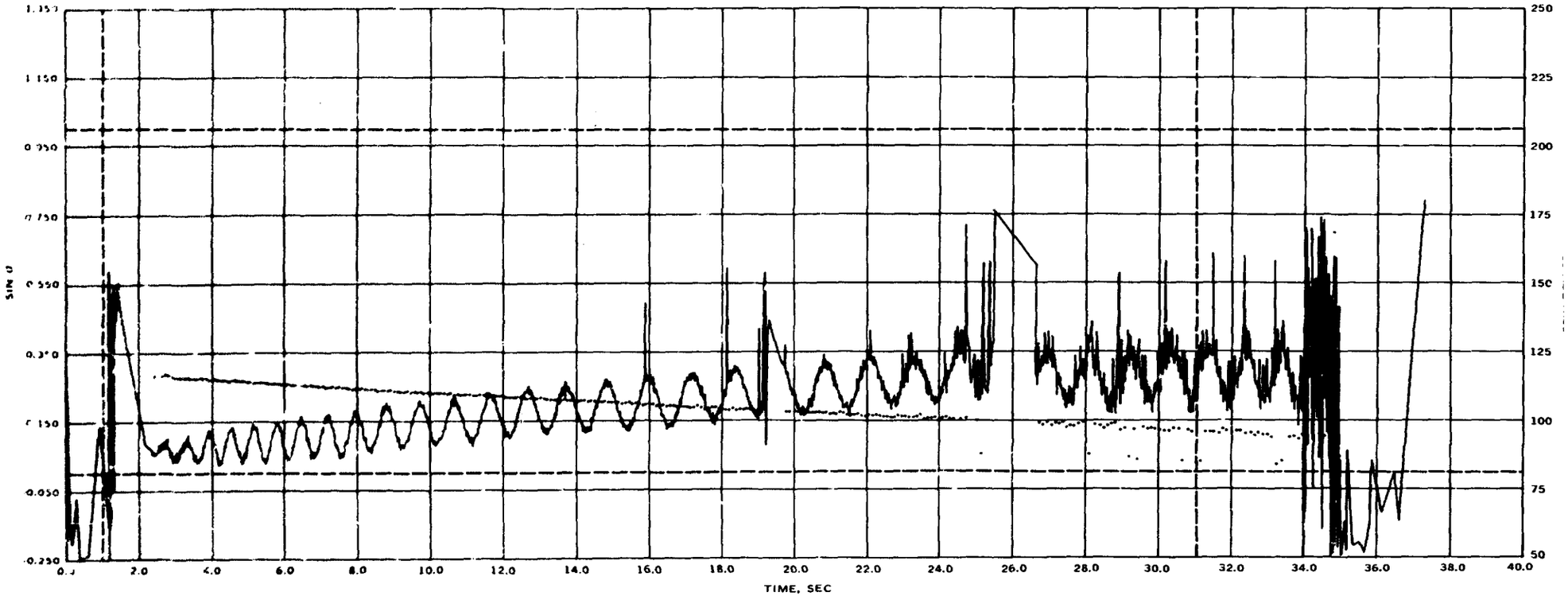

C.

PLATE I. (Contd.)
C. Yaw sonde record.
D. Computer simulation of yaw sonde record.

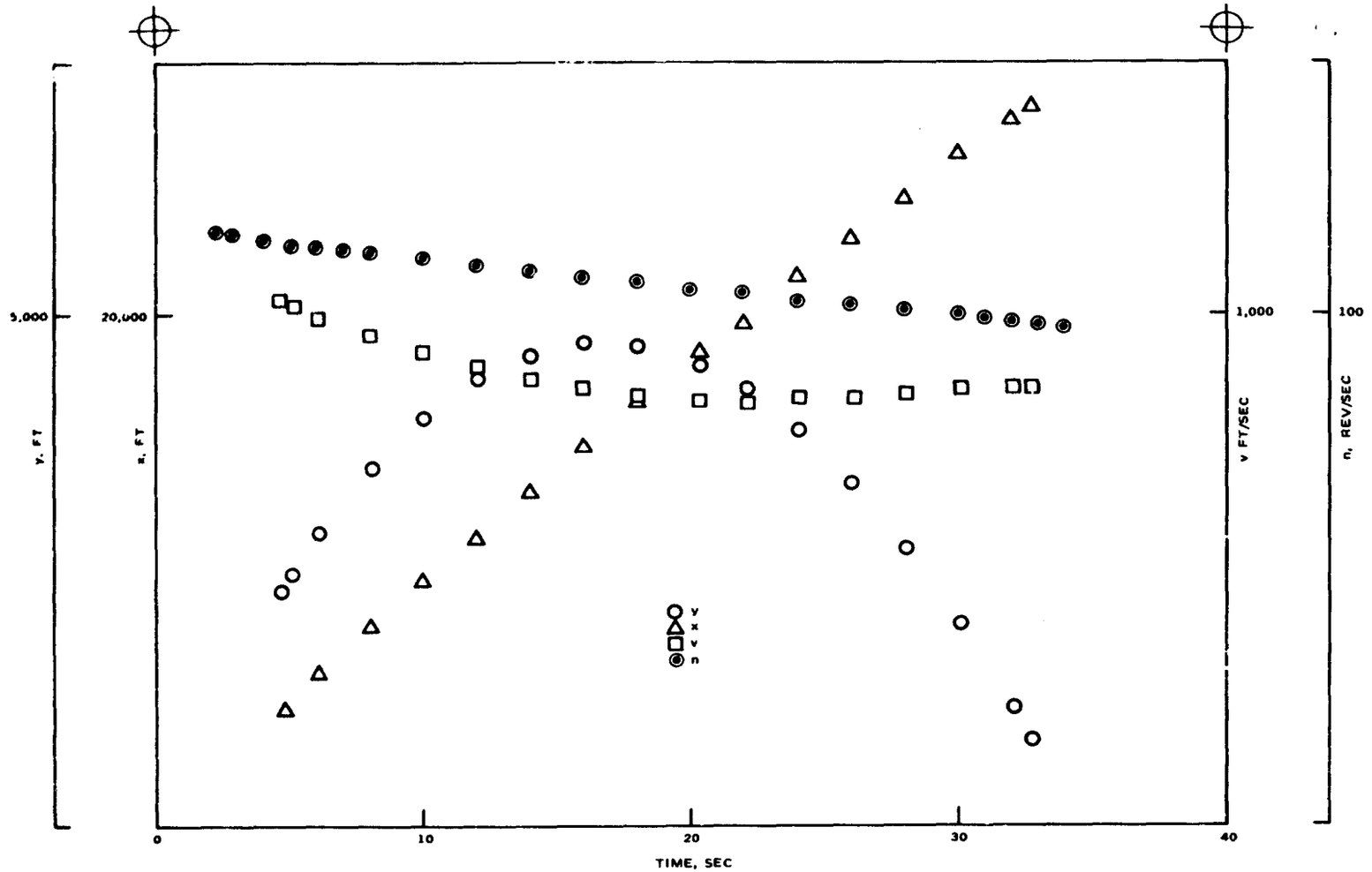

A.

PLATE II. E-7274A, Round 5.
A. Trajectory data.
B. Computed trajectory elements.

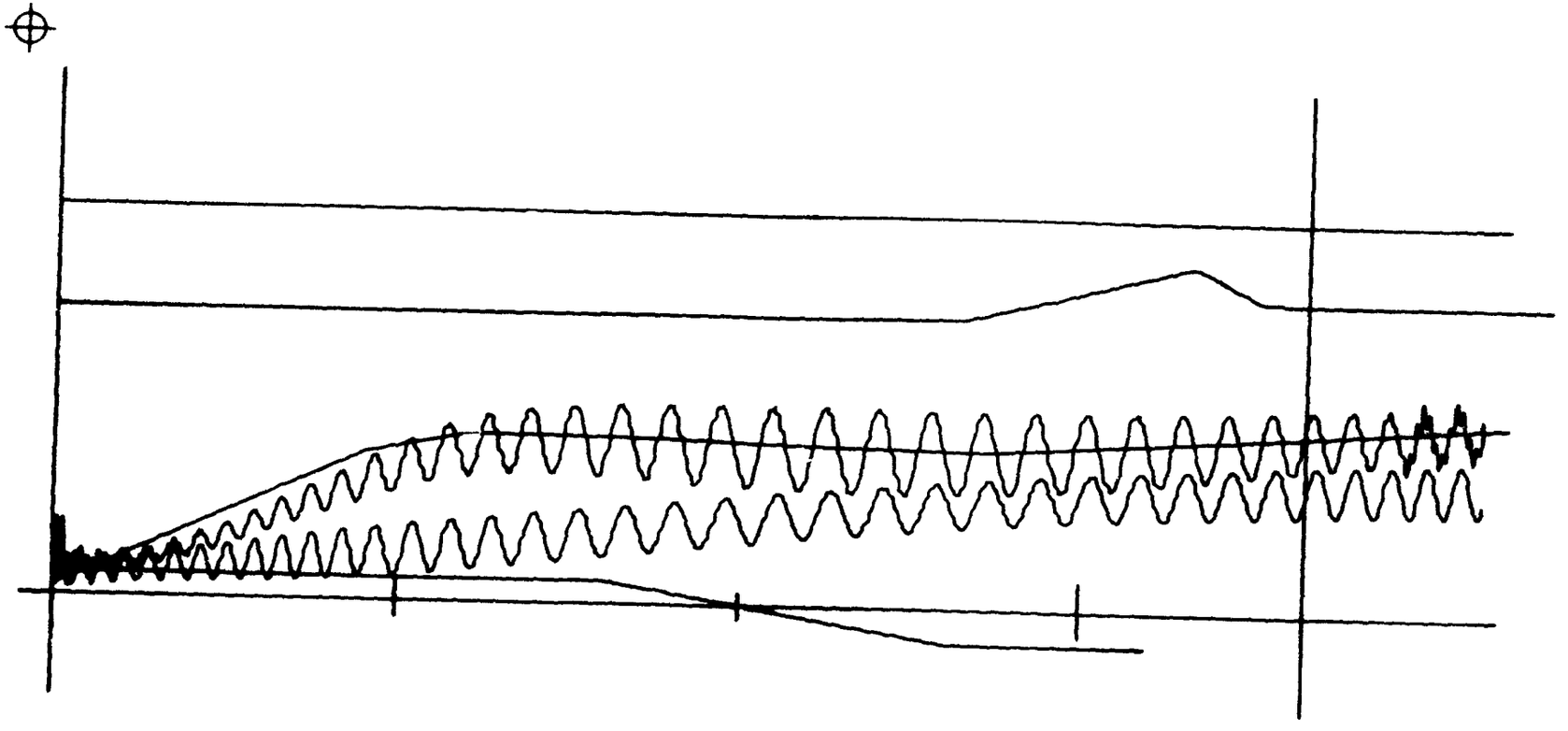

D.

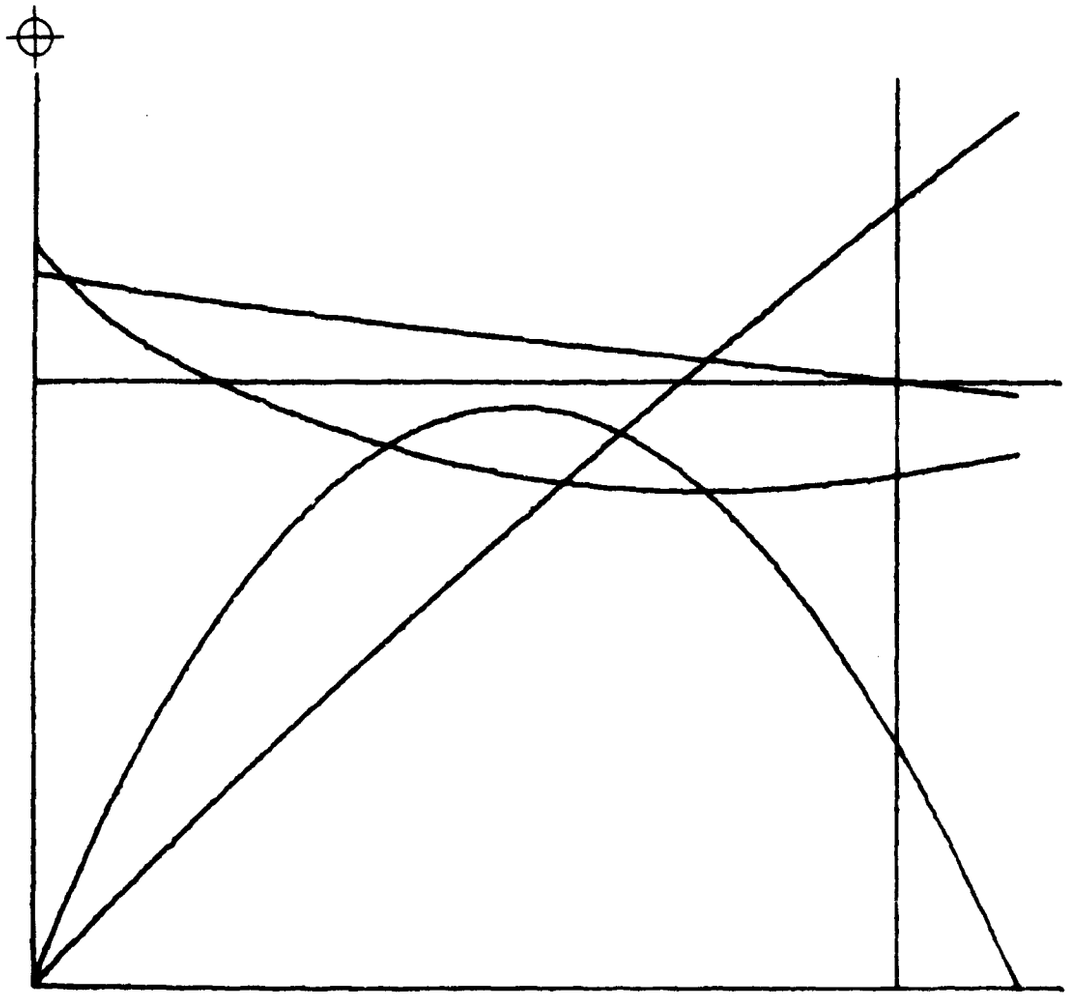

B.

D.

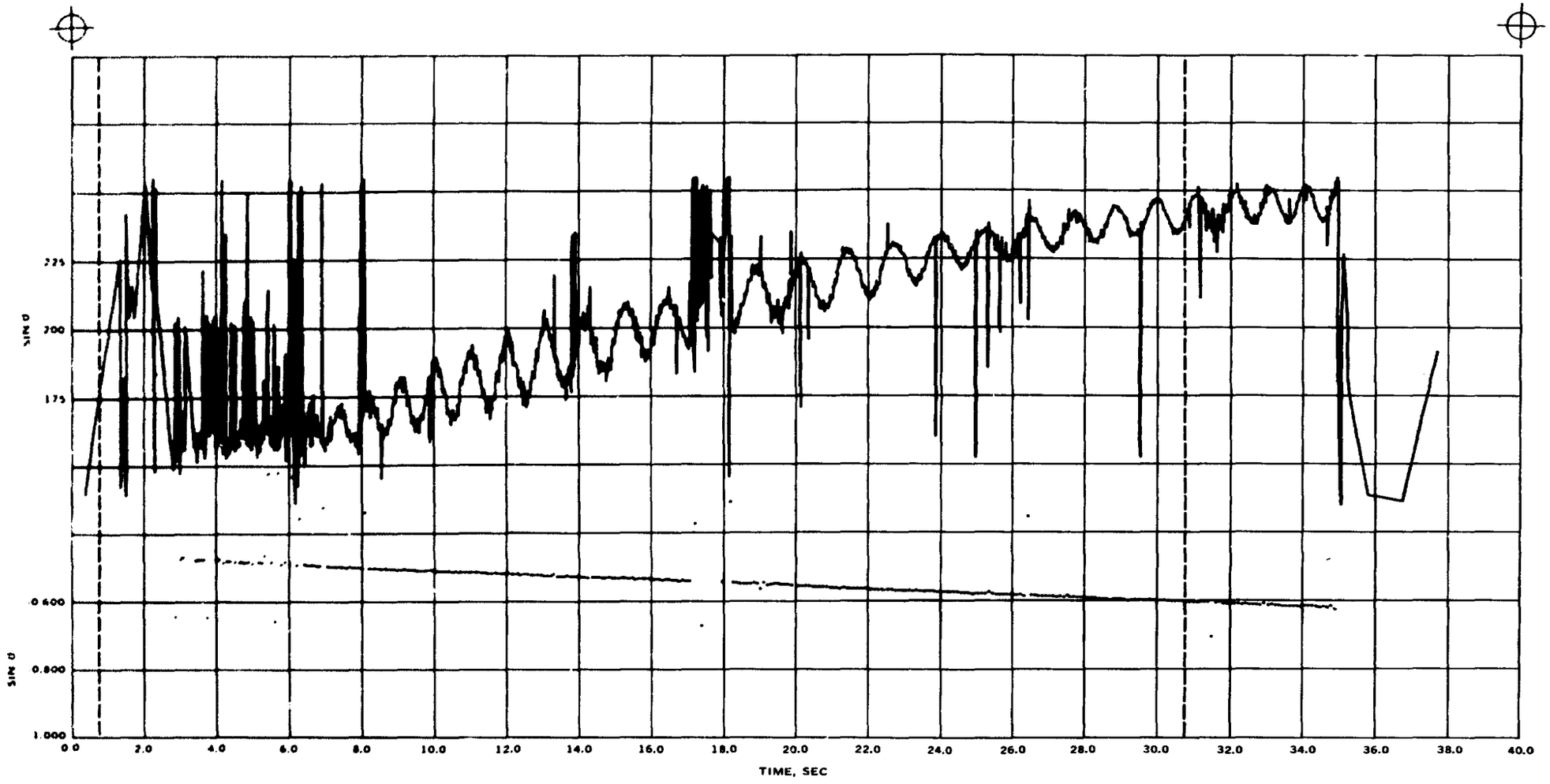

C.

PLATE II. (Contd.)
C. Yaw sonde record.
D. Computer simulation of yaw sonde record.

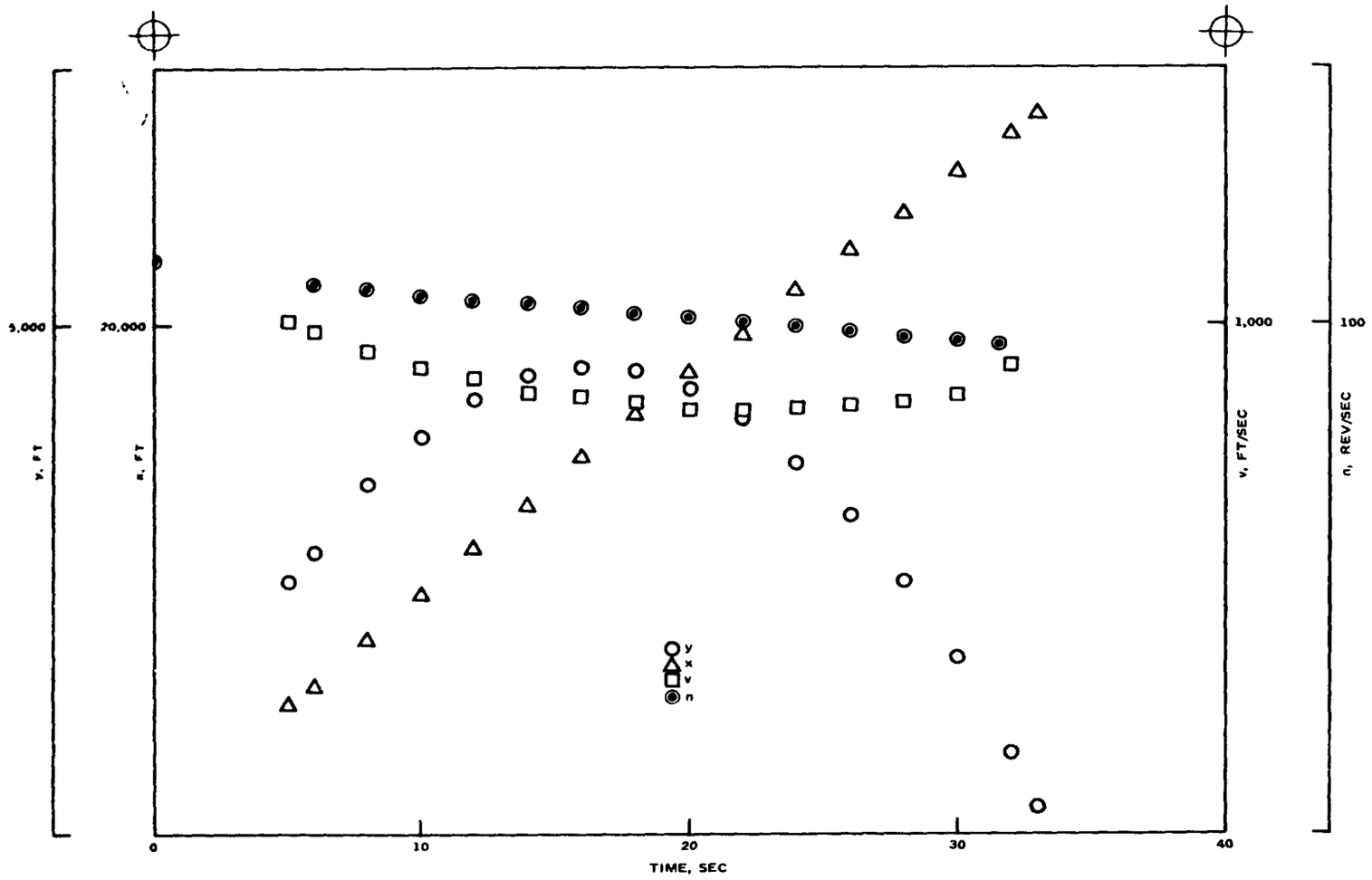

A.

PLATE III. E-7274A, Round 7.
A. Trajectory data.
B. Computed trajectory elements.

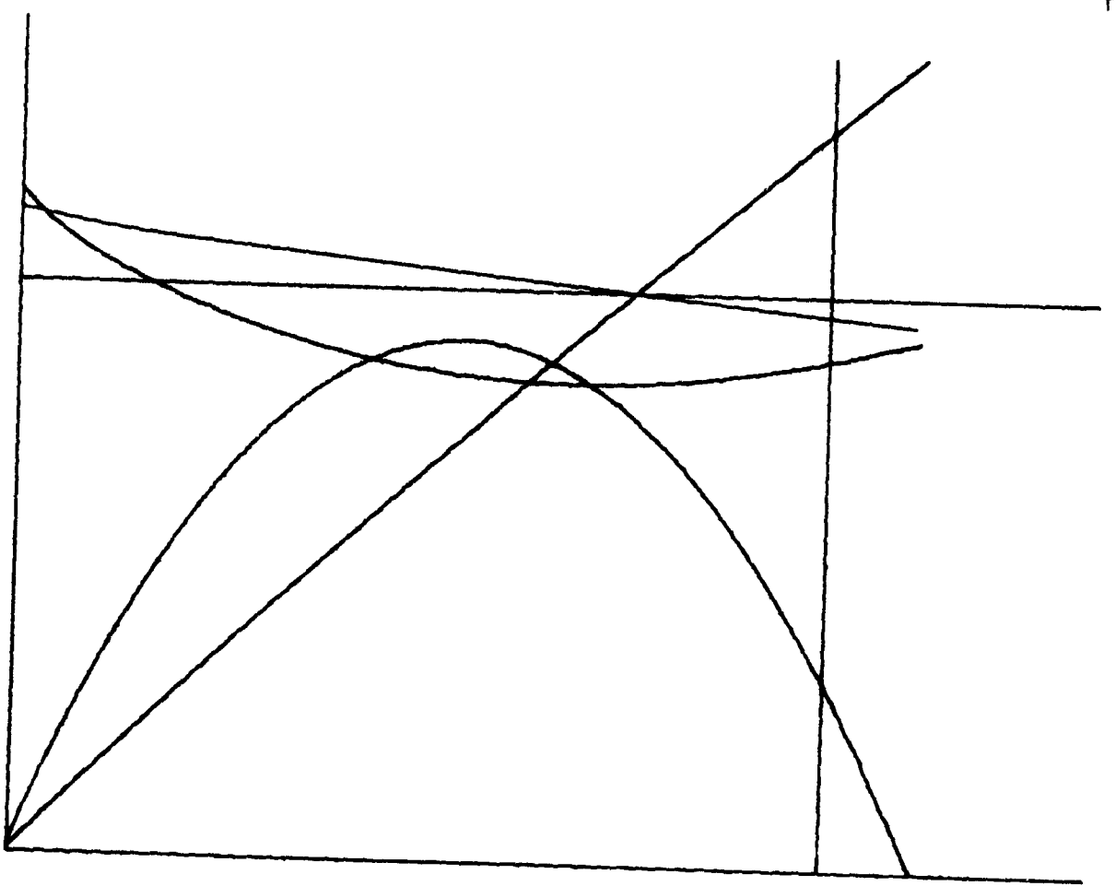

B.

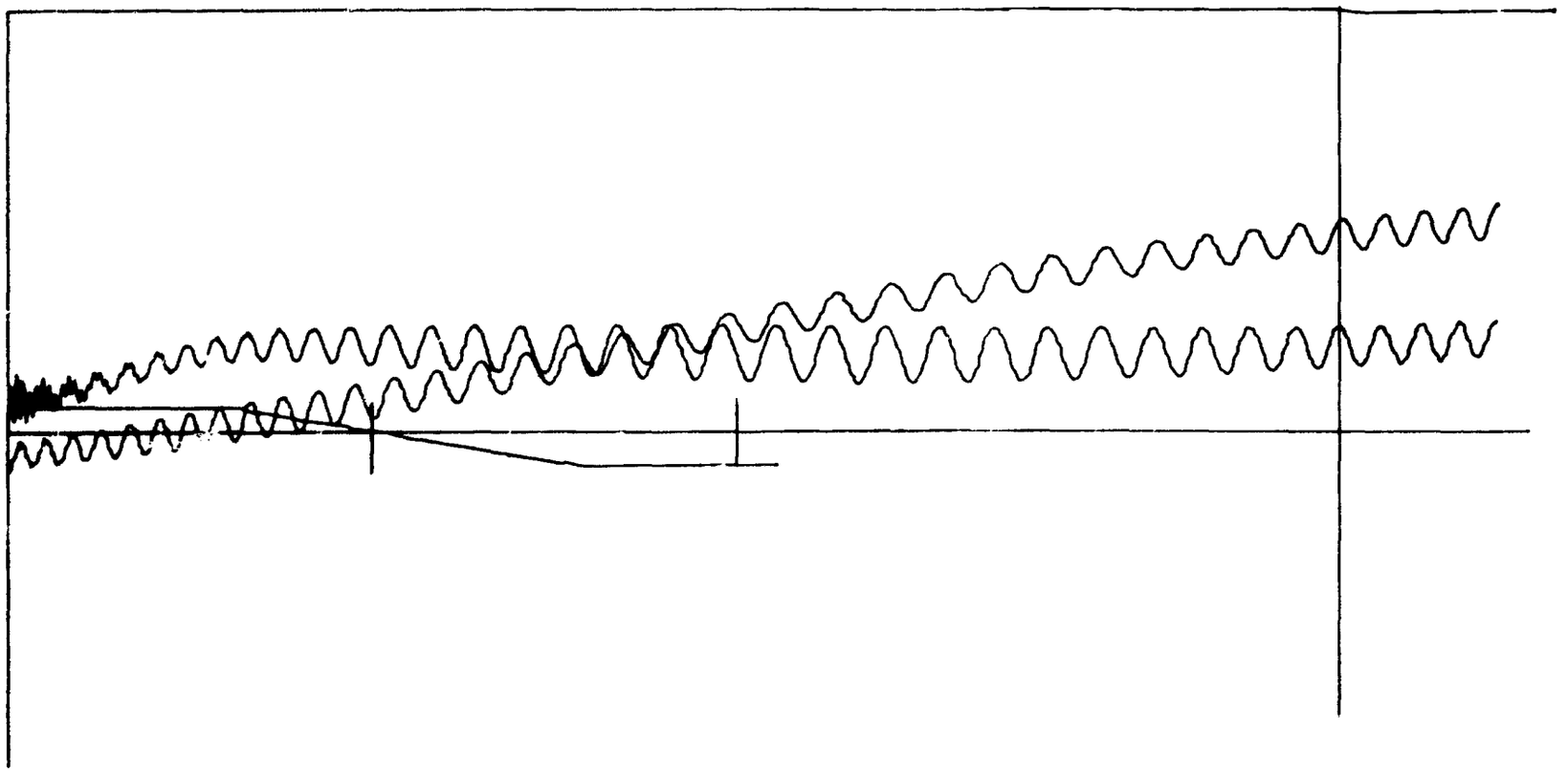

D.

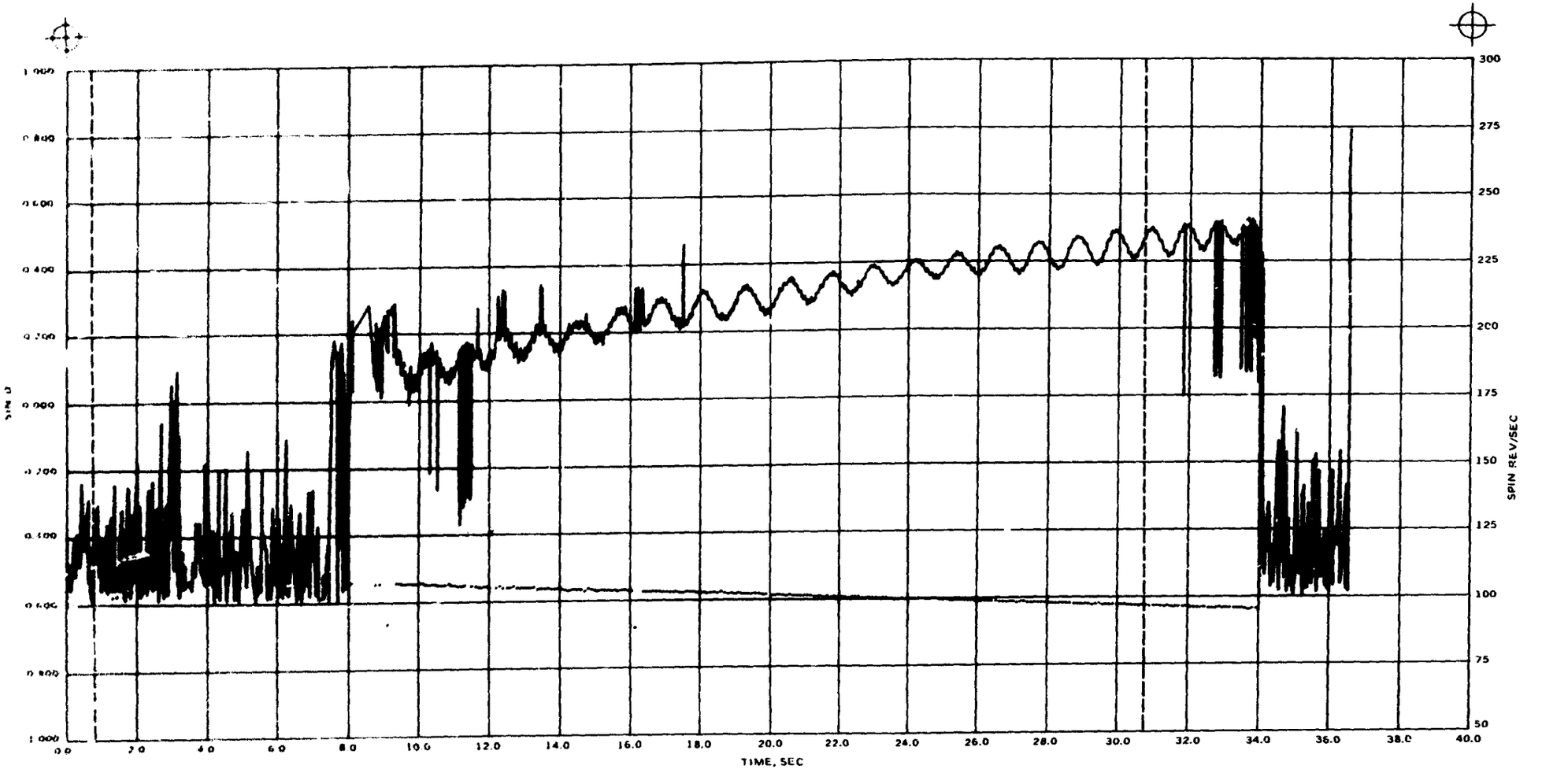

C.

PLATE III. (Contd.)
C. Yaw sonde record.
D. Computer simulation of yaw sonde record.

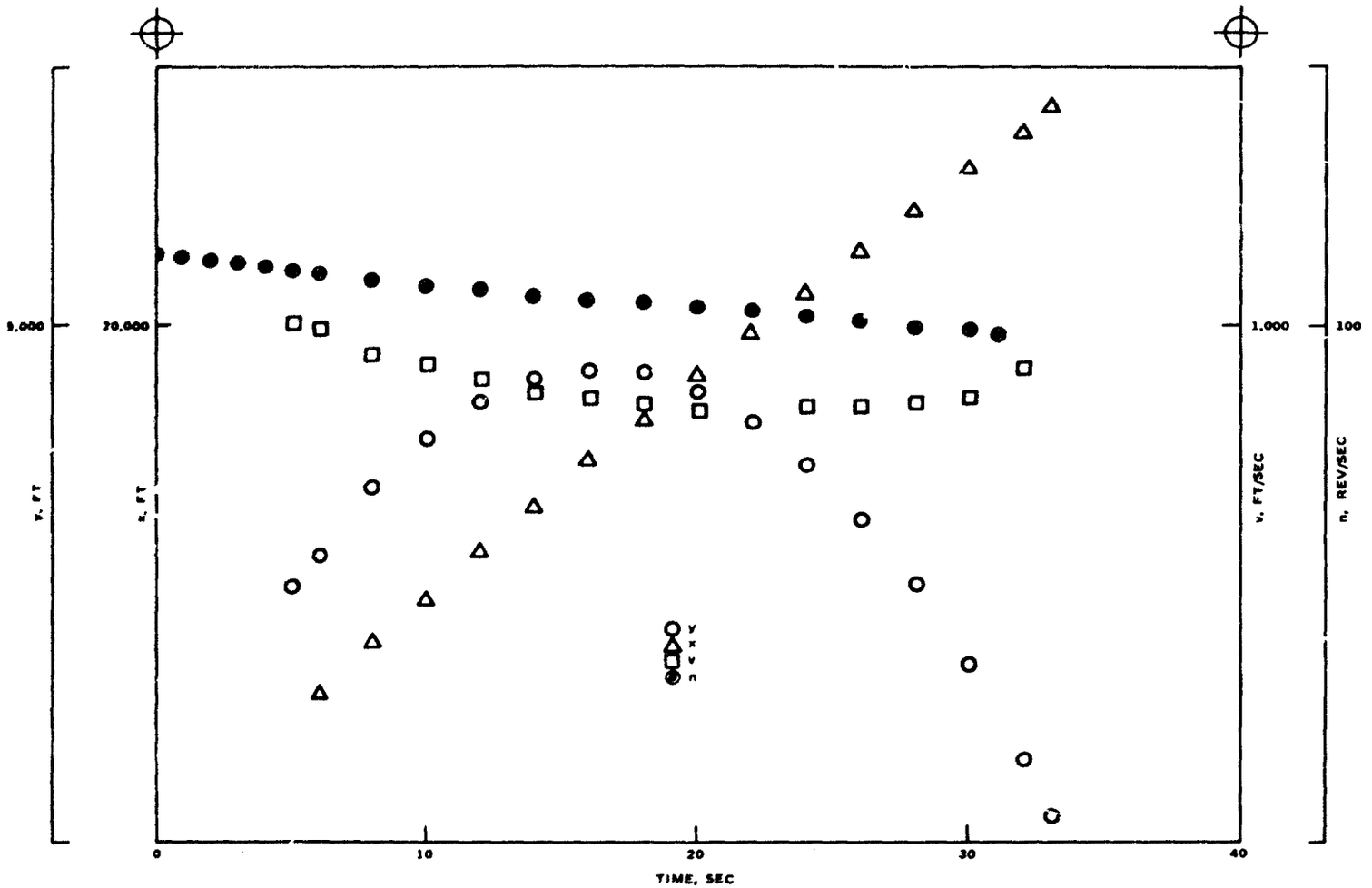

A.

PLATE IV. E-7274A, Round 8.
A. Trajectory data.
B. Computed trajectory elements.

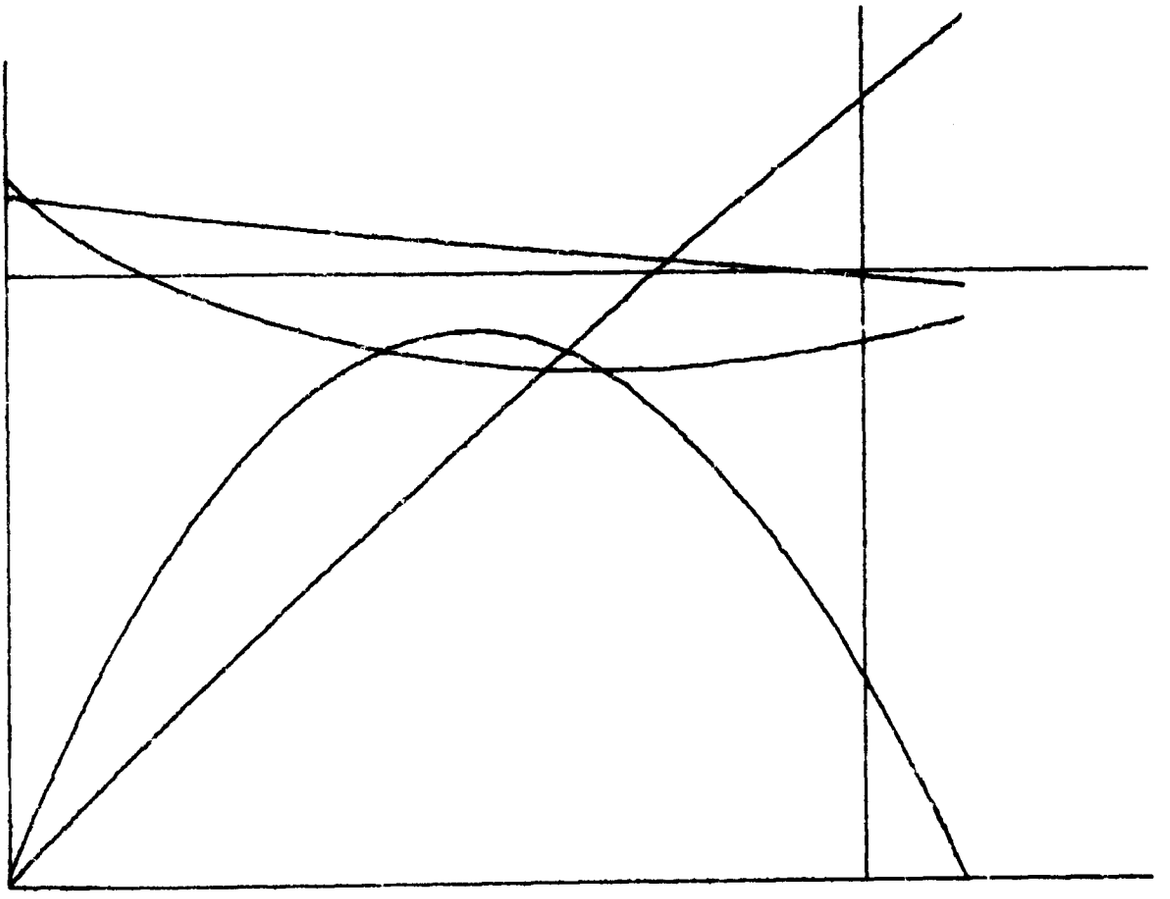

B.

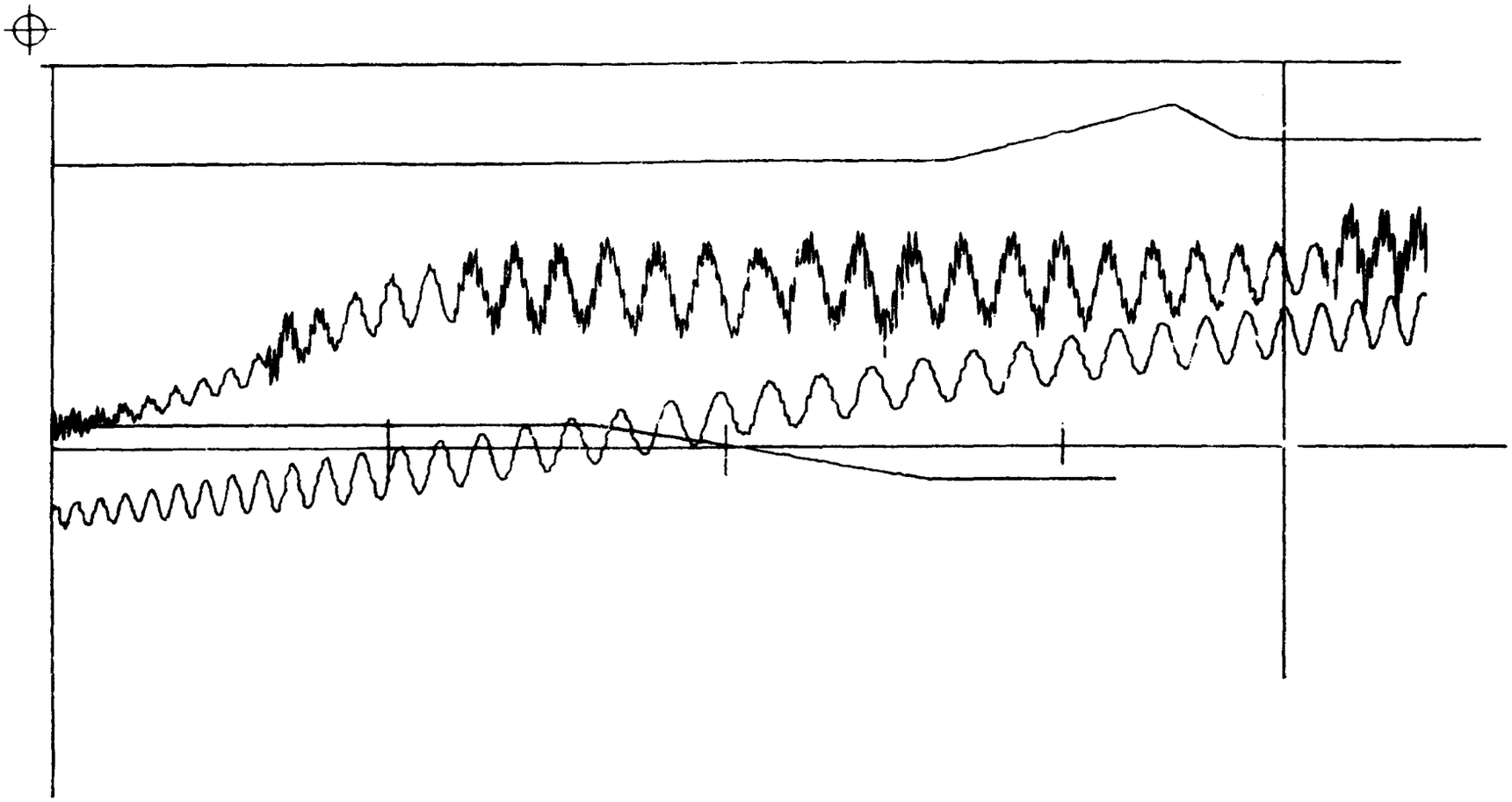

D.

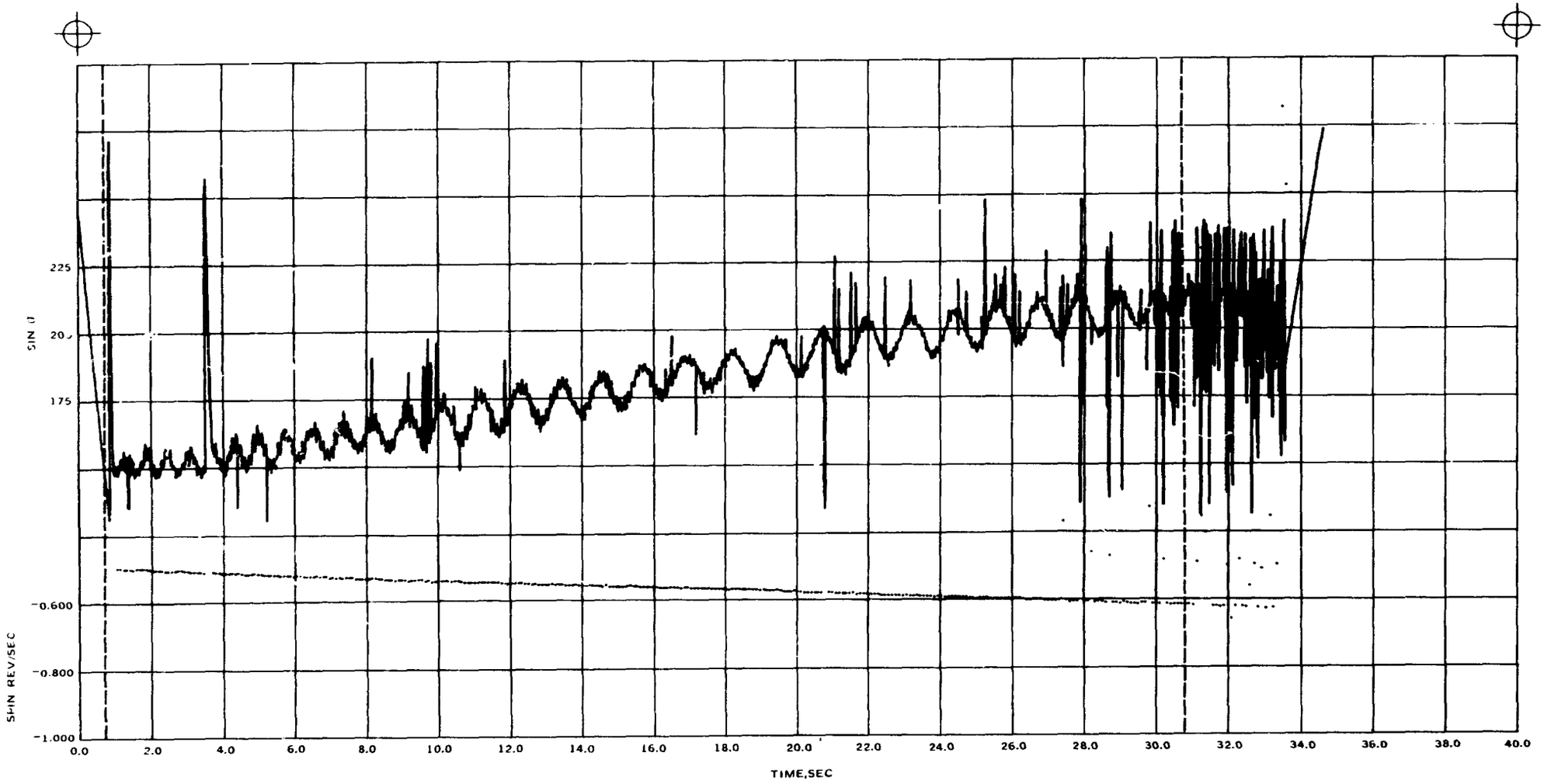

C.

PLATE IV. (Contd.)
C. Yaw sonde record.
D. Computer simulation of yaw sonde record.

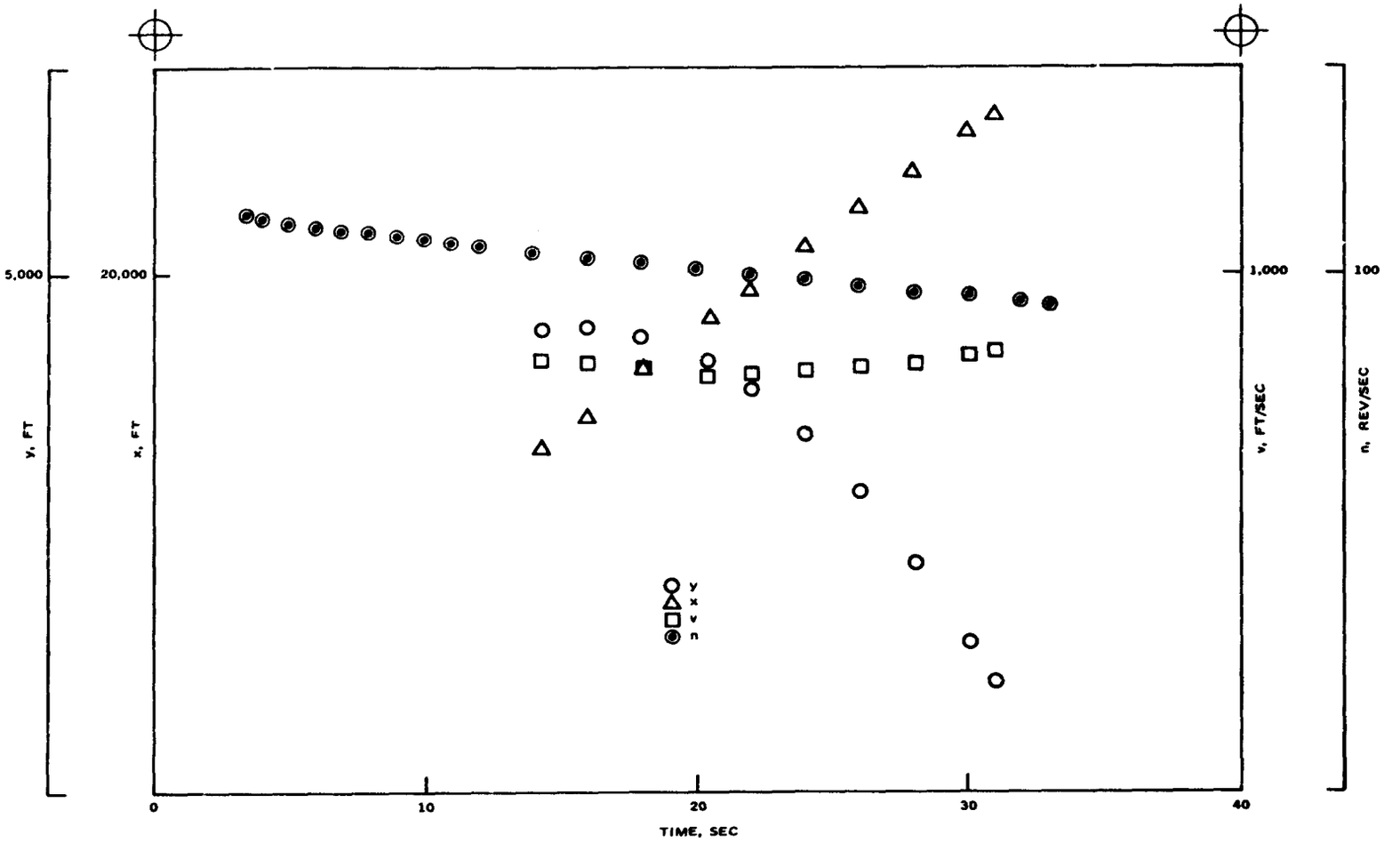

A.

PLATE V. E-7274A, Round 10.
A. Trajectory data.
B. Computed trajectory elements.

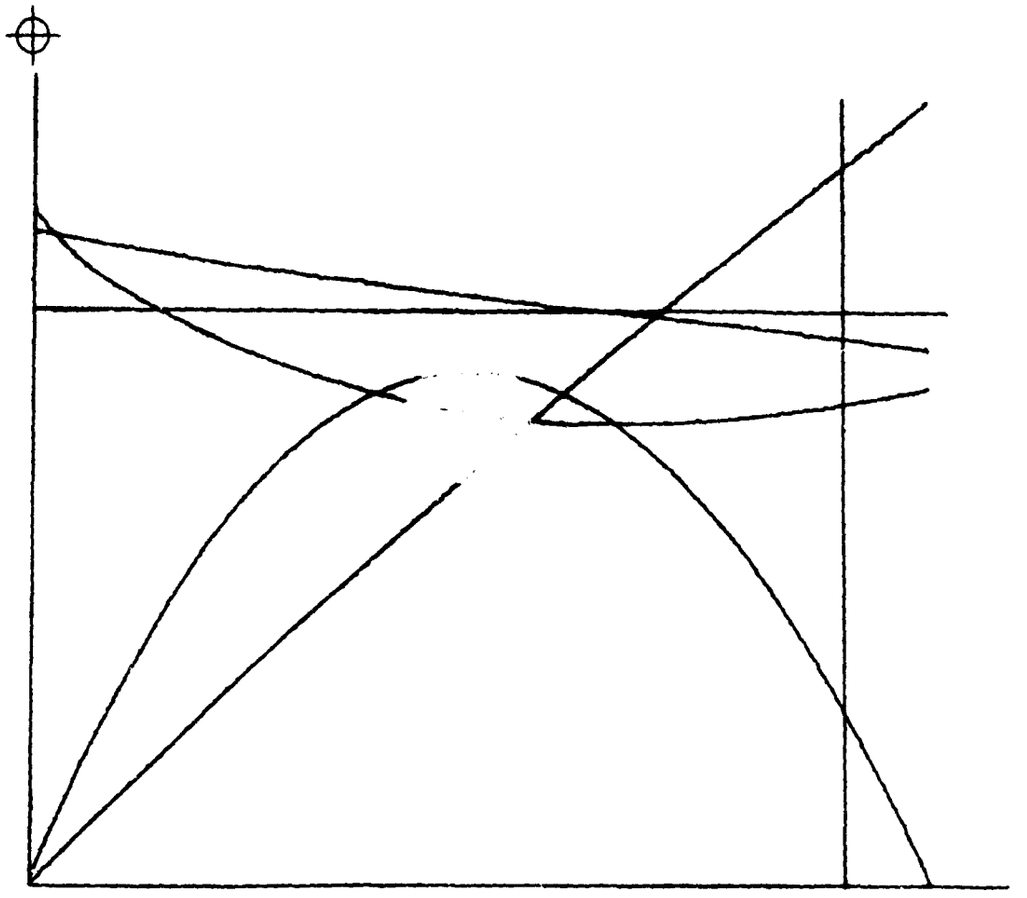

B.

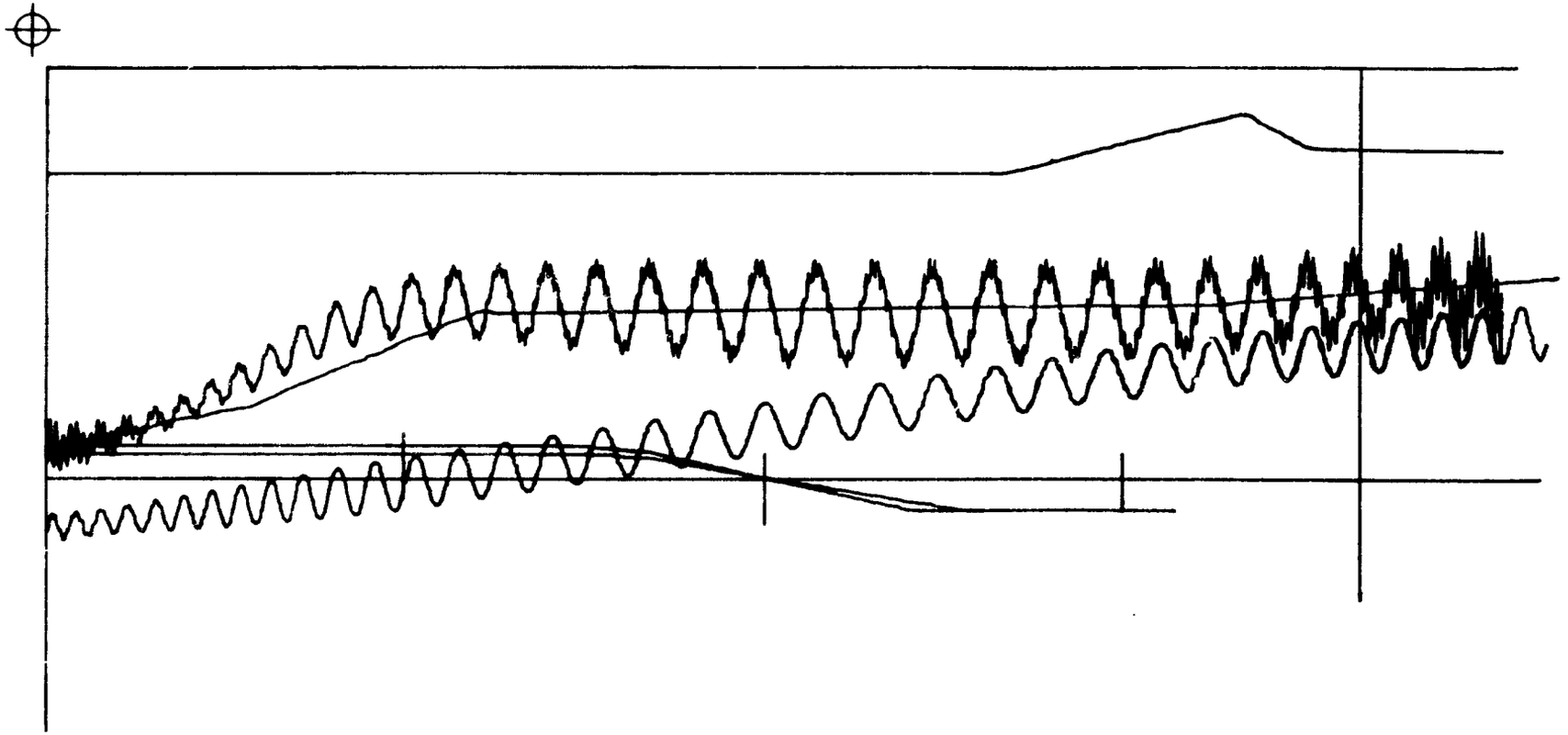

D.

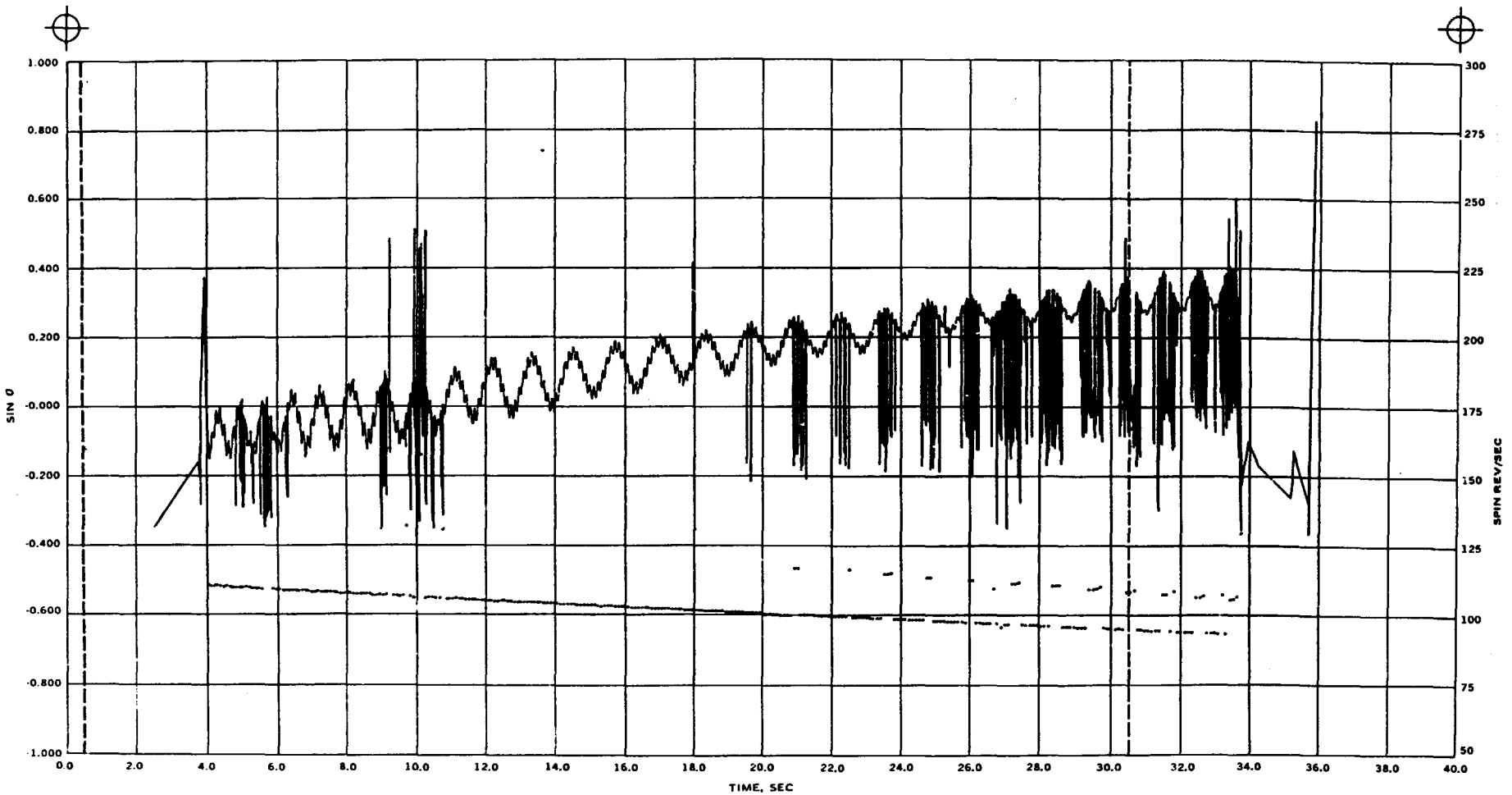

C.

PLATE V. (Contd.)
C. Yaw *sonde record.*
D. Computer simulation of yaw sonde record.

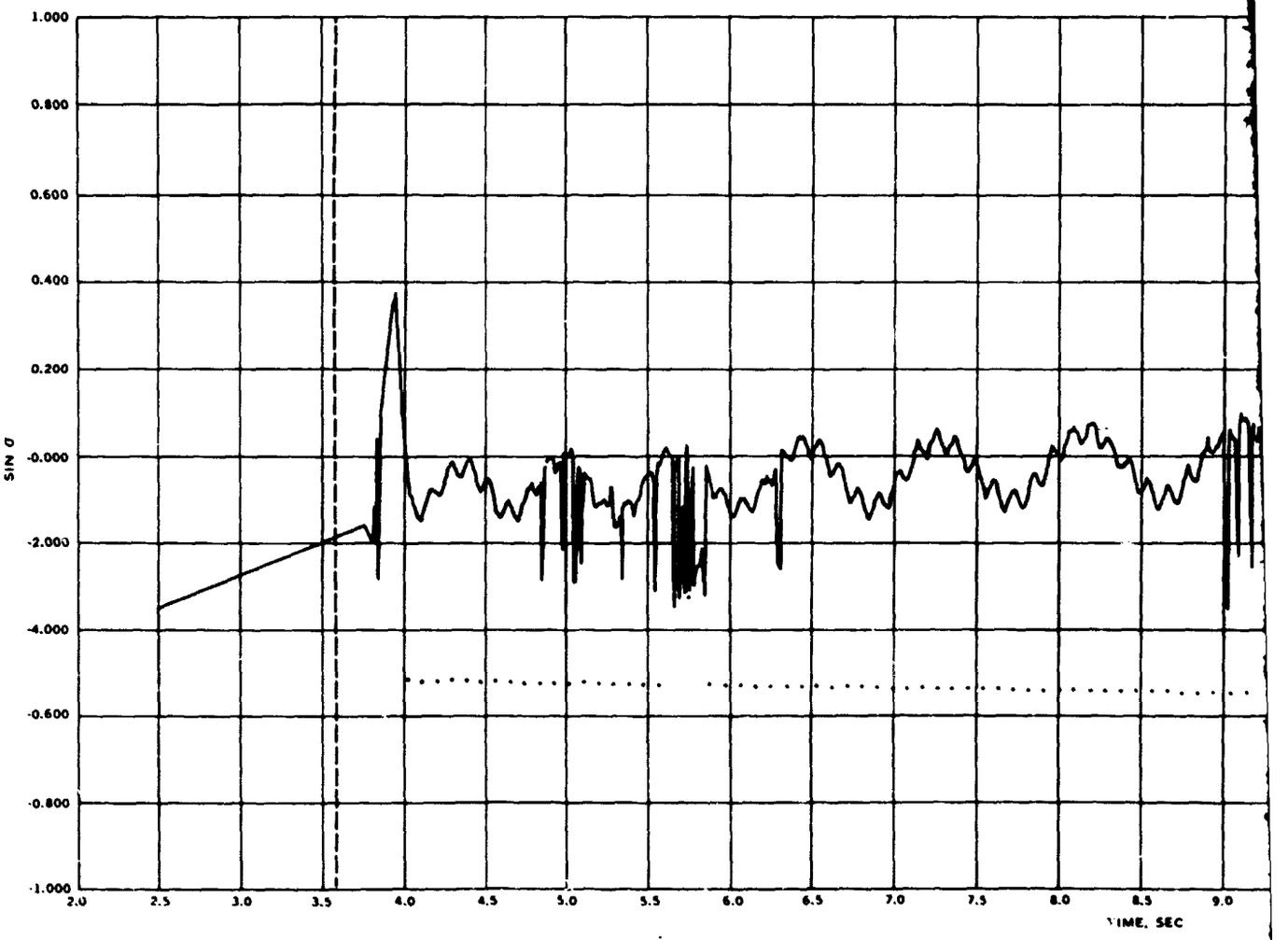

E.

PLATE V. (Contd.)
E. Yaw sonde record, expanded time scale.
F. Computer simulation of yaw sonde record, expanded tim

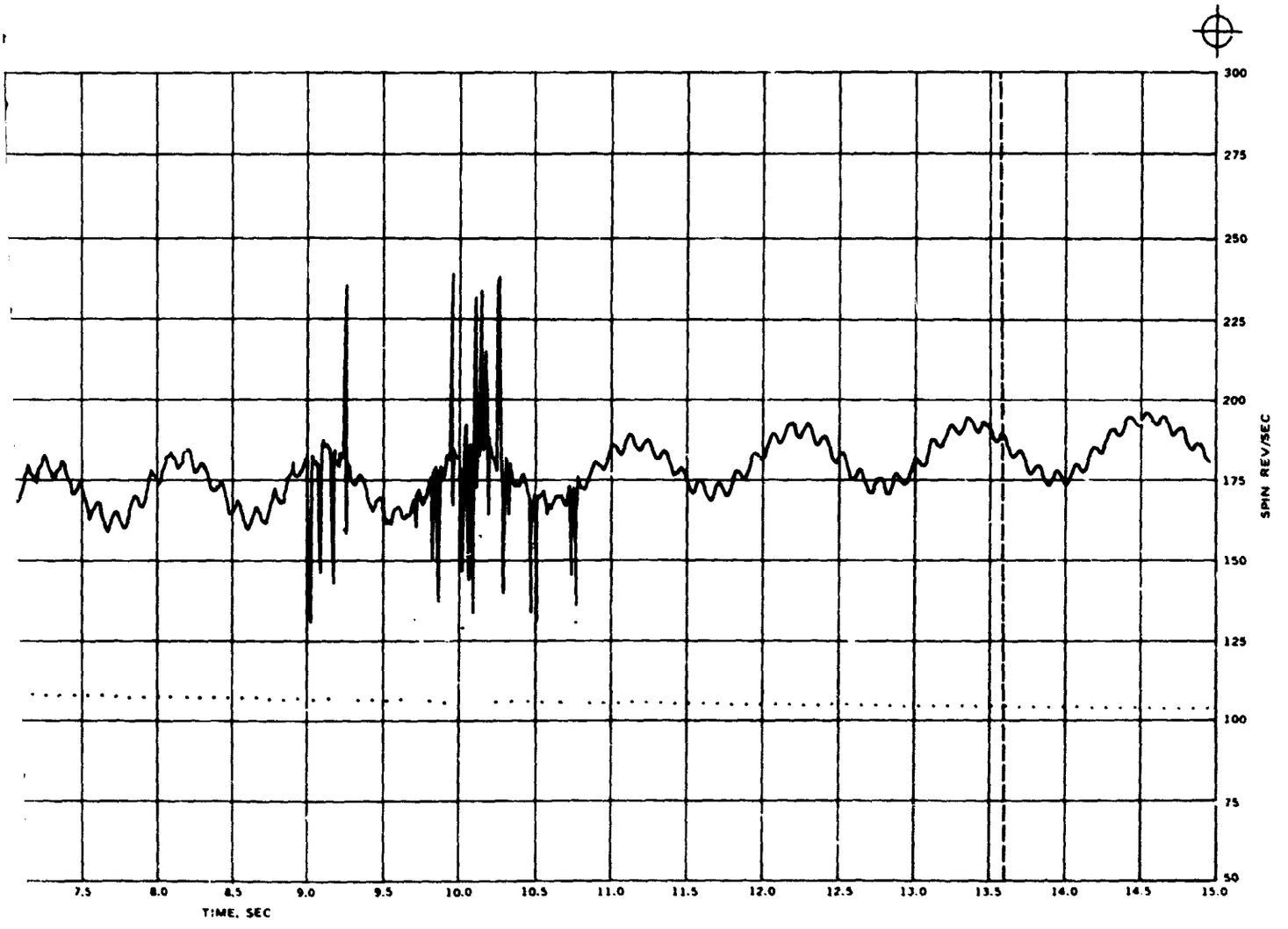

E.

ord, expanded time scale.
lation of yaw sonde record, expanded time scale.

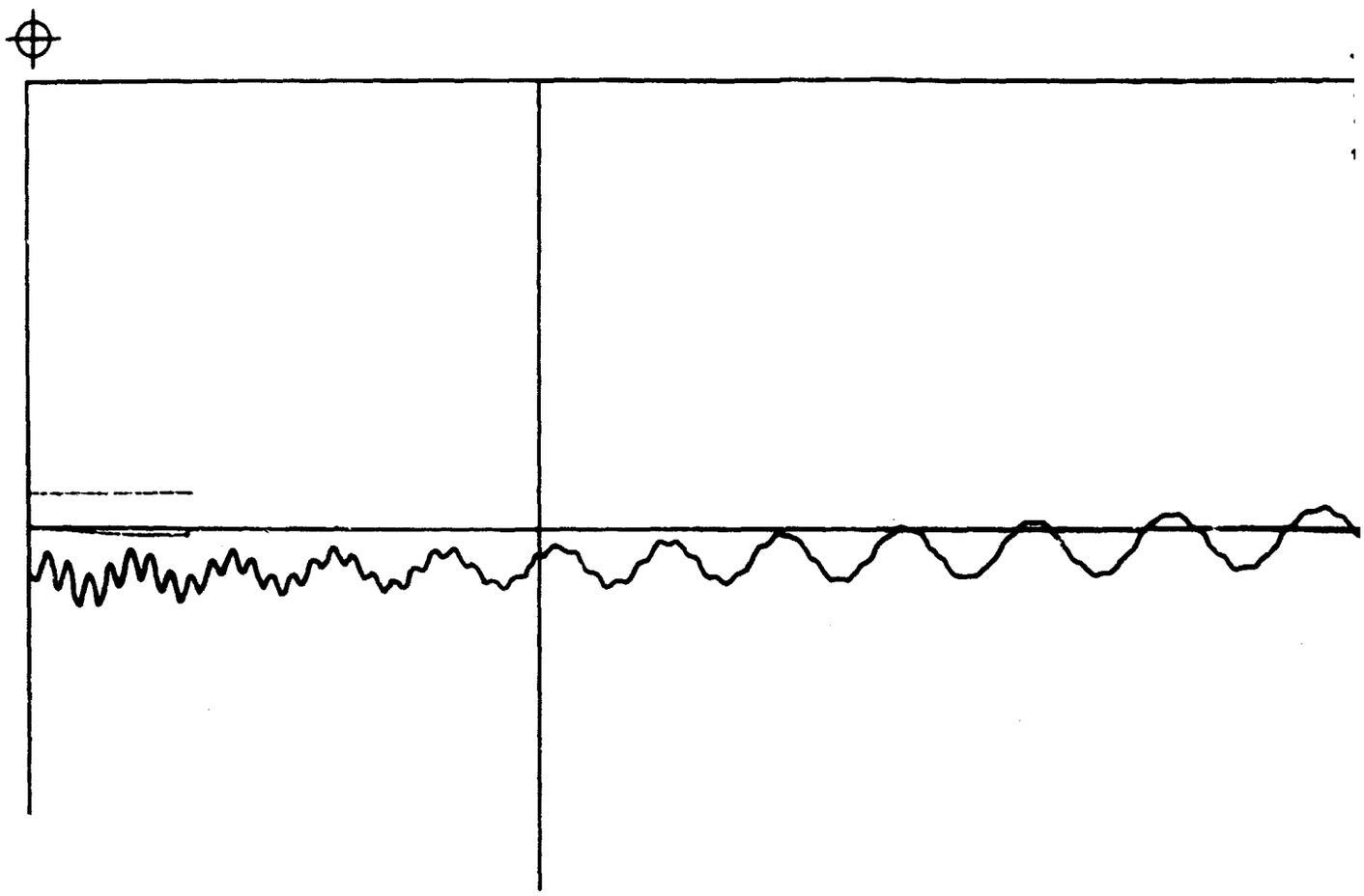

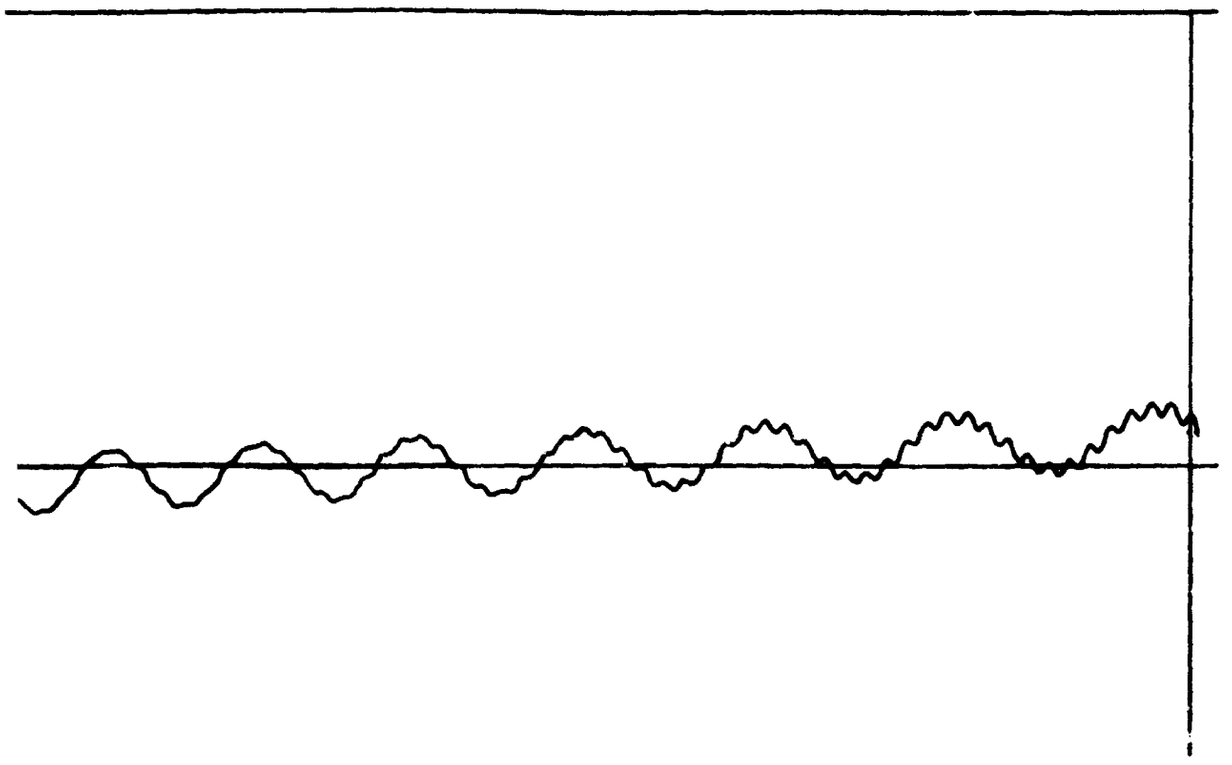

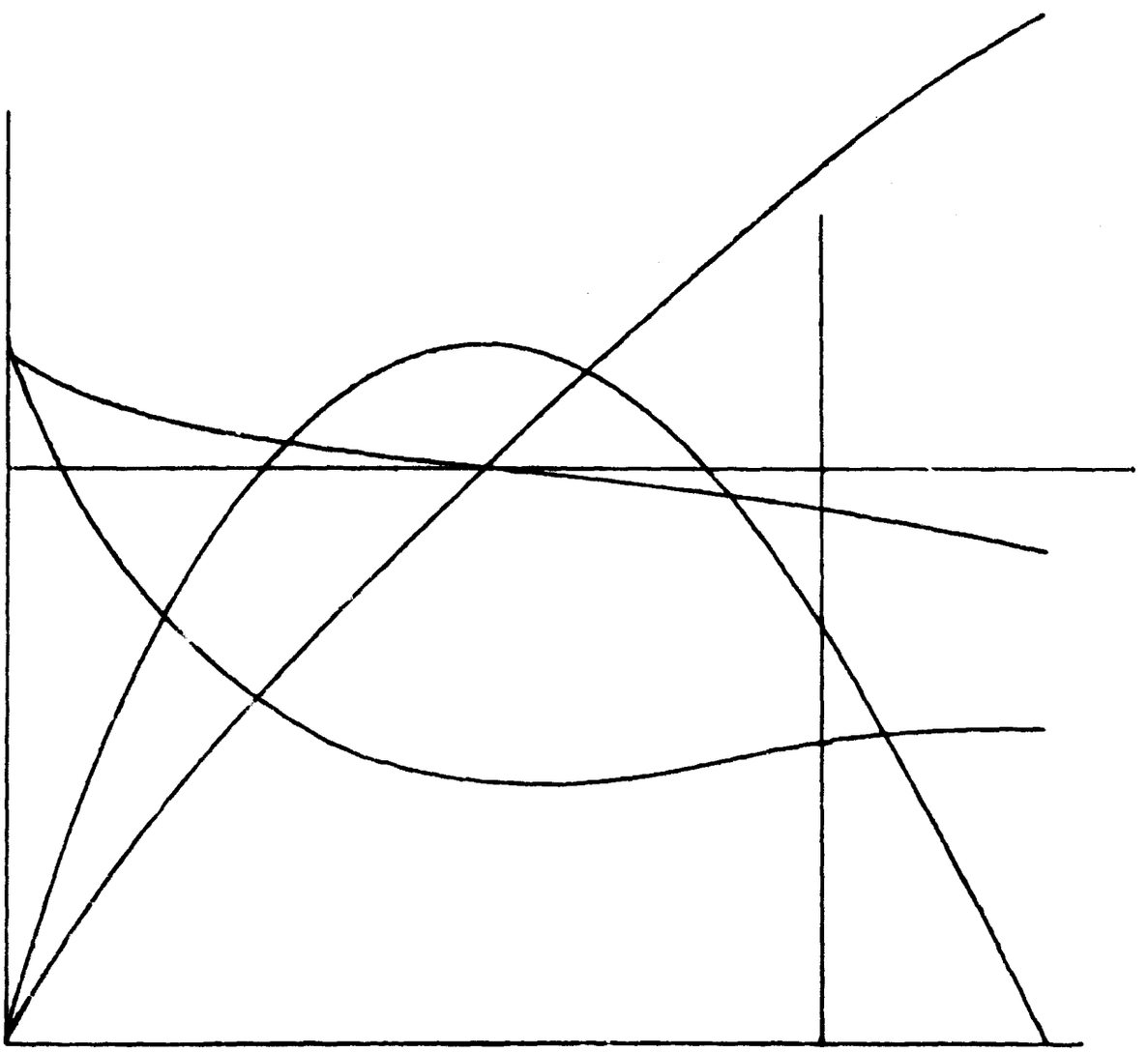

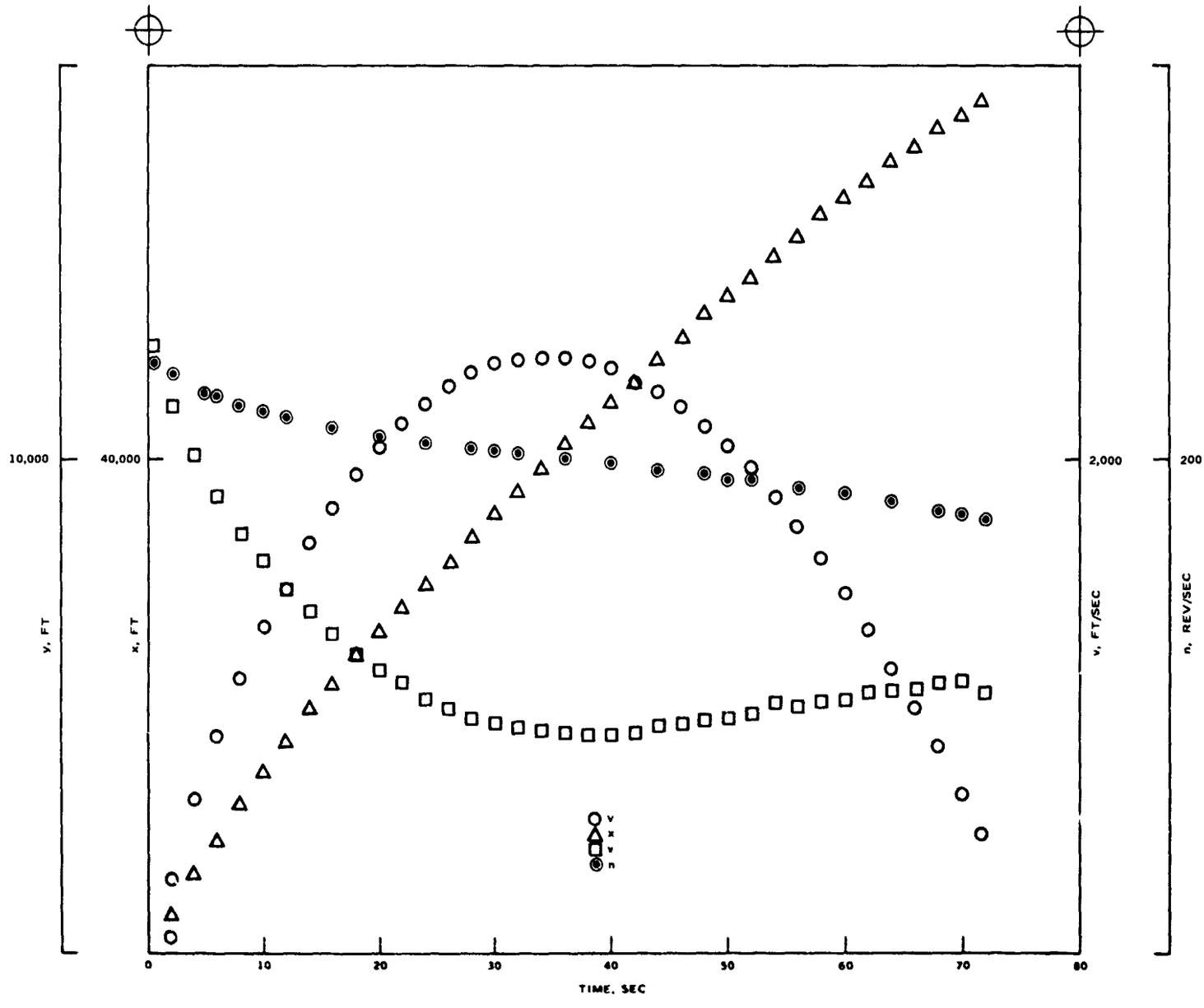

A.

PLATE VI. E-7274B, Round 8.
A. Trajectory data.
B. Computed trajectory elements.

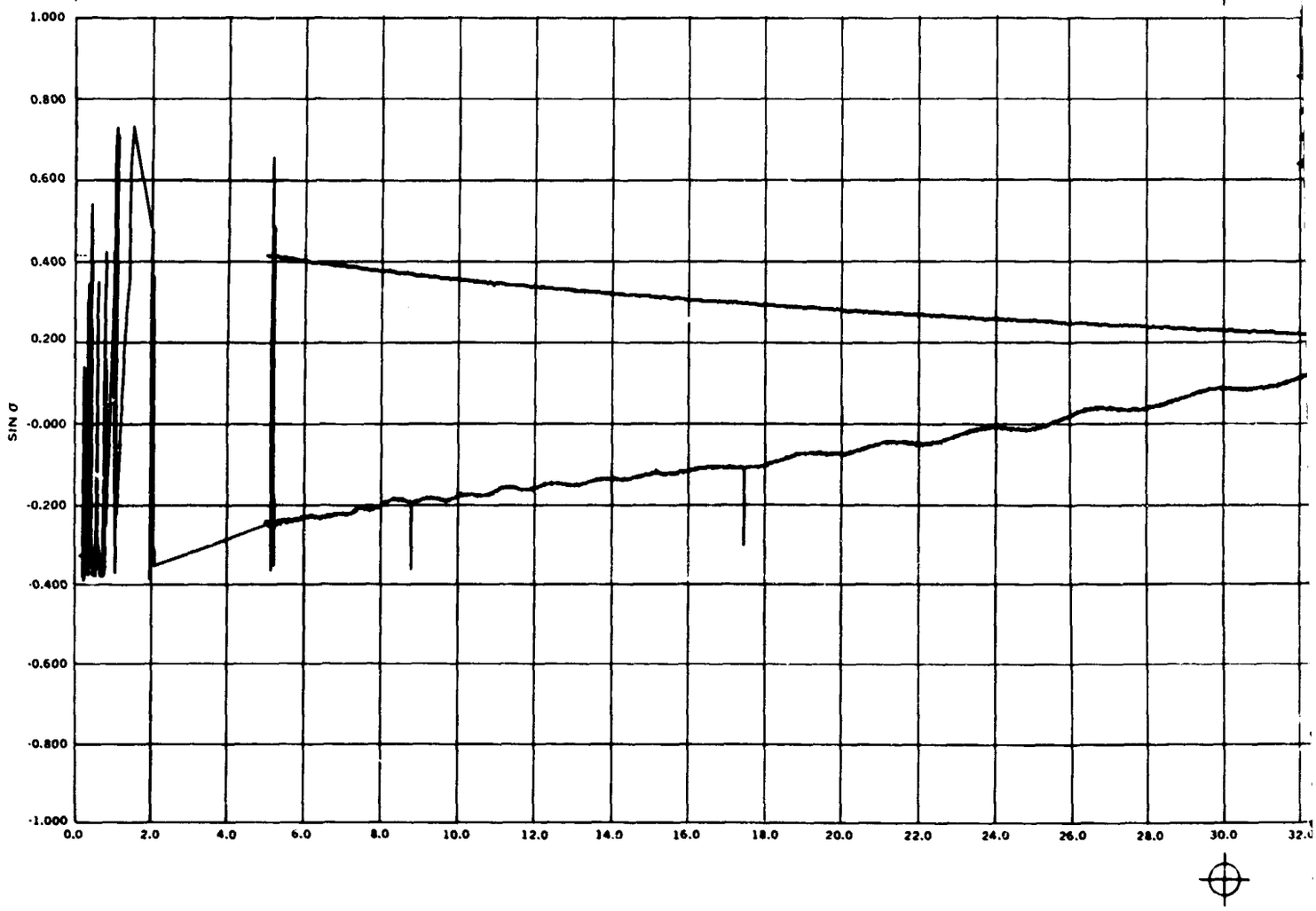
1.000
0.800
0.600
0.400
0.200
-0.000
-0.200
-0.400
-0.600
-0.800
-1.000
SIN σ
0.0
2.0
4.0
6.0
8.0
10.0
12.0
14.0
16.0
18.0
20.0
22.0
24.0
26.0
28.0
30.0

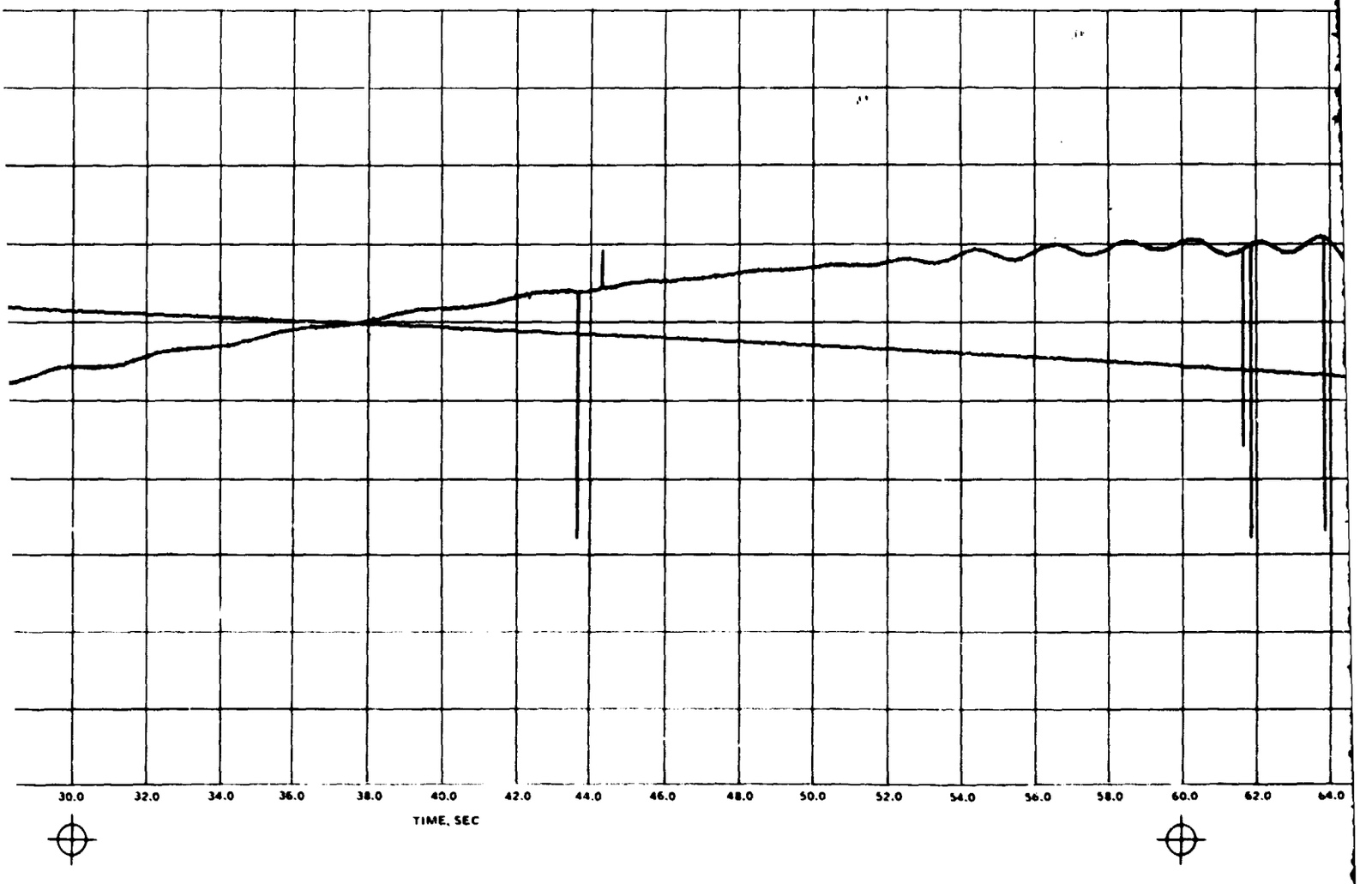

C.

PLATE VI. (Contd.)

C. Yaw sonde record.

D. Computer simulation of yaw sonde record; projectile disturbed at 47.8 sec.

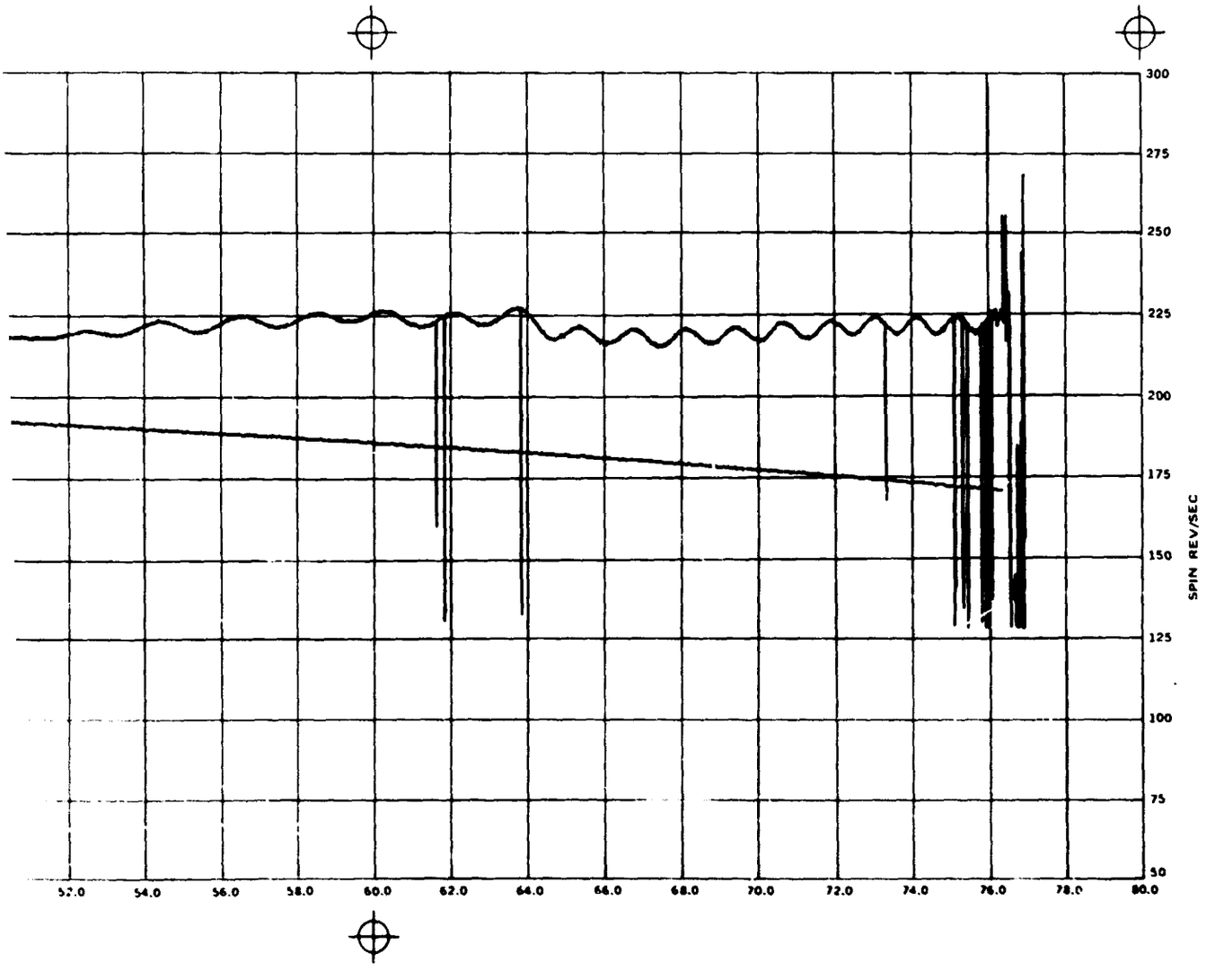
300
275
250
225
200
175
150
125
100
75
50
SPIN REV/SEC
52.0
54.0
56.0
58.0
60.0
62.0
64.0
66.0
68.0
70.0
72.0
74.0
76.0
78.0
80.0

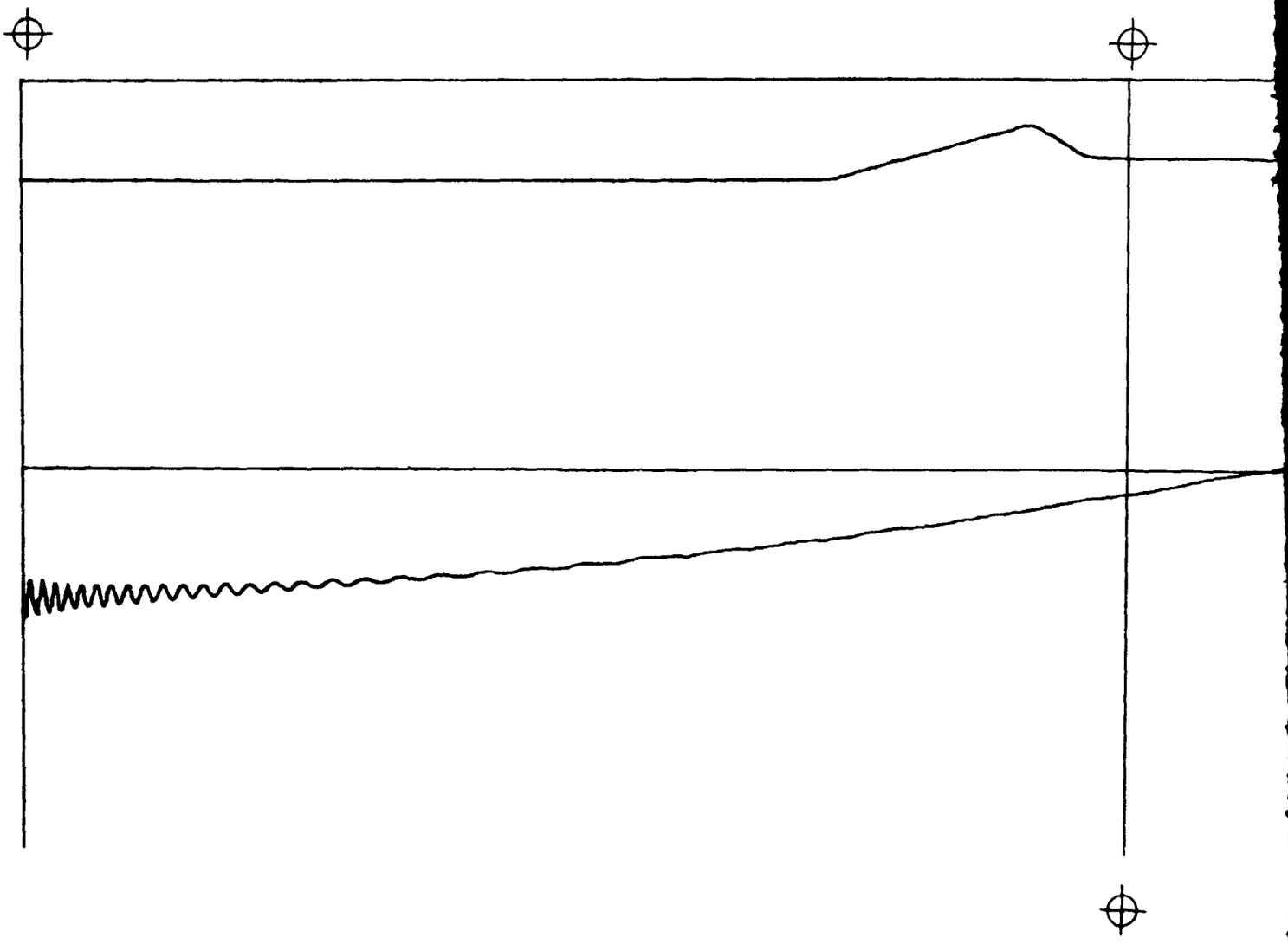

A

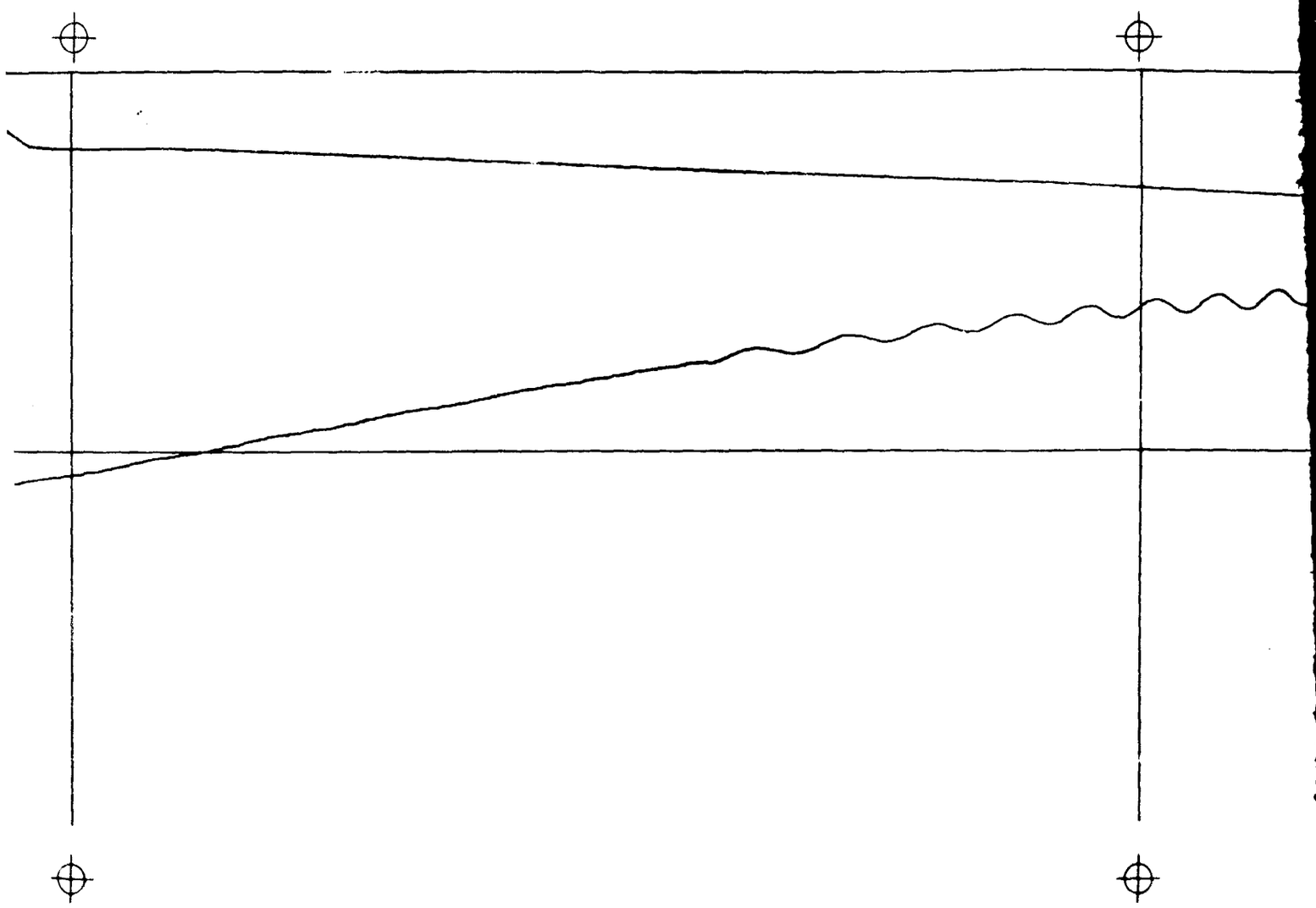

D.

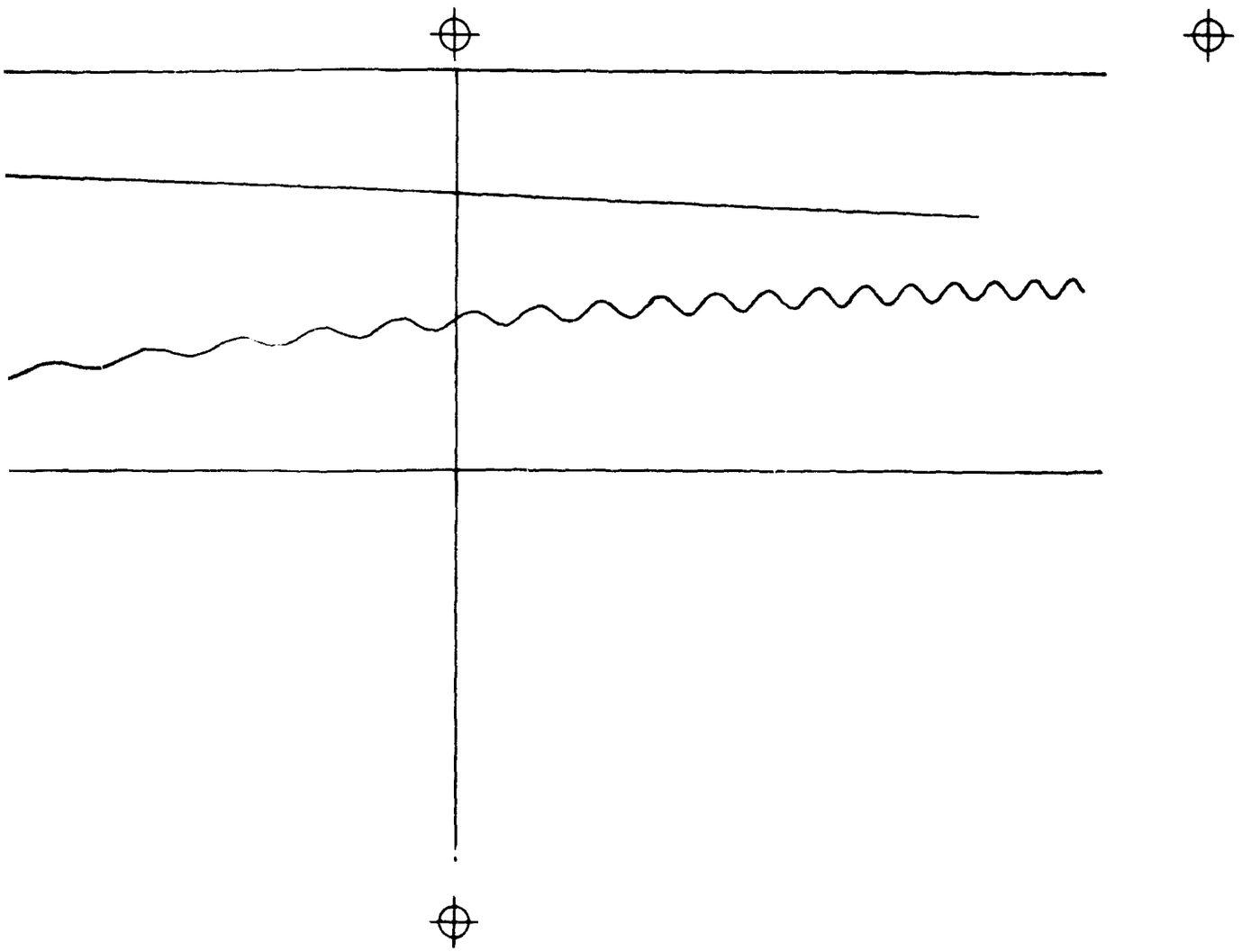

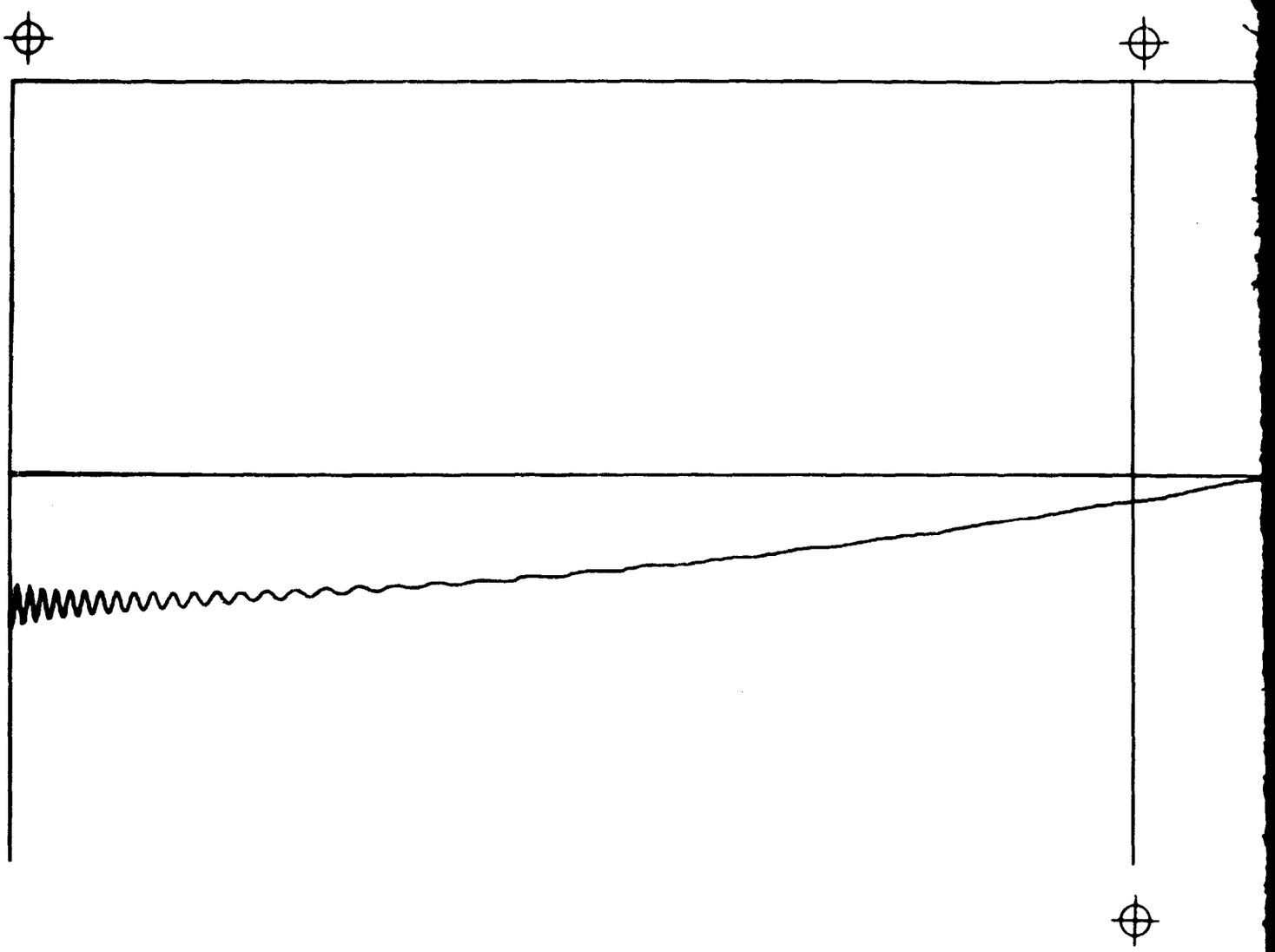

A

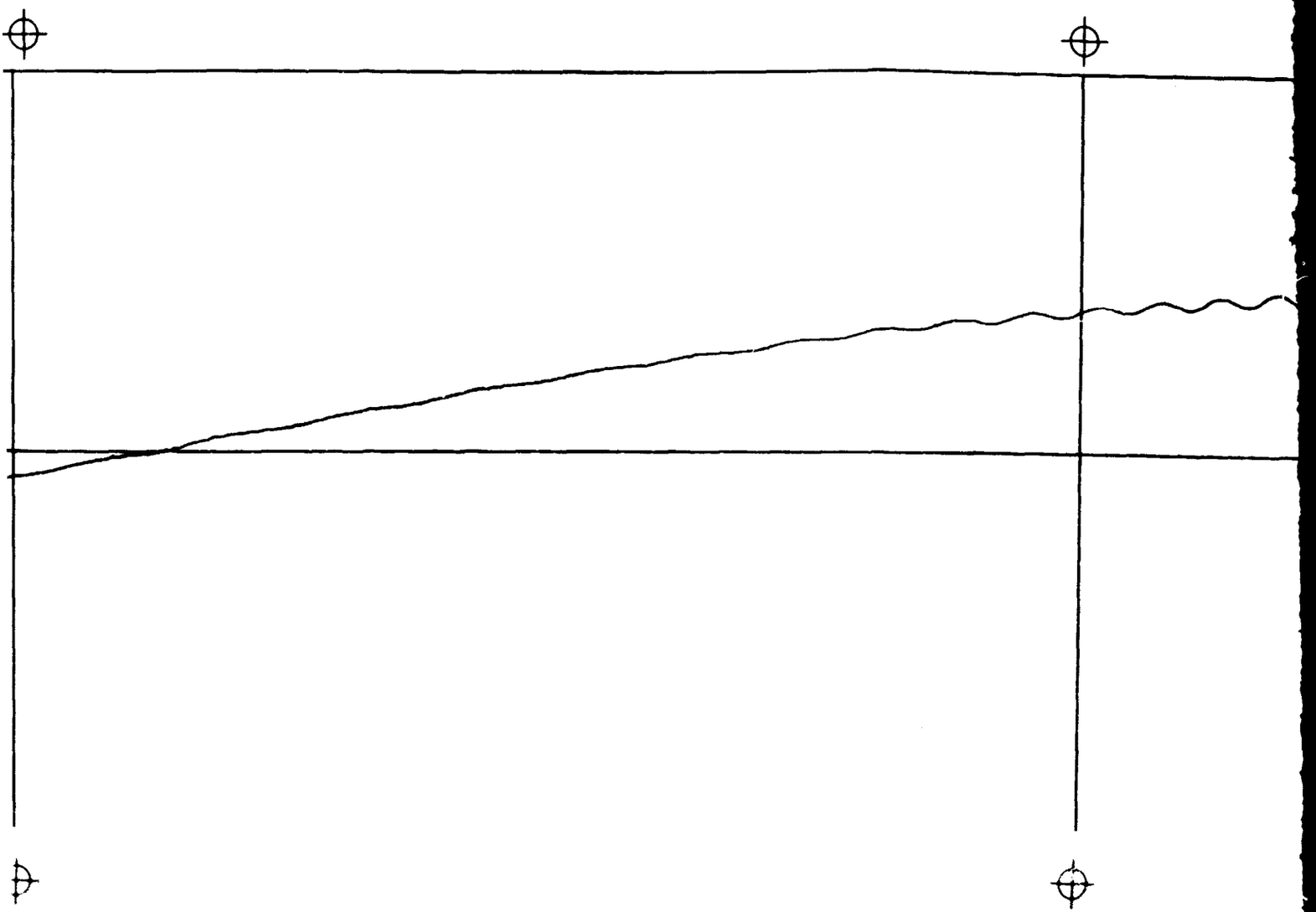

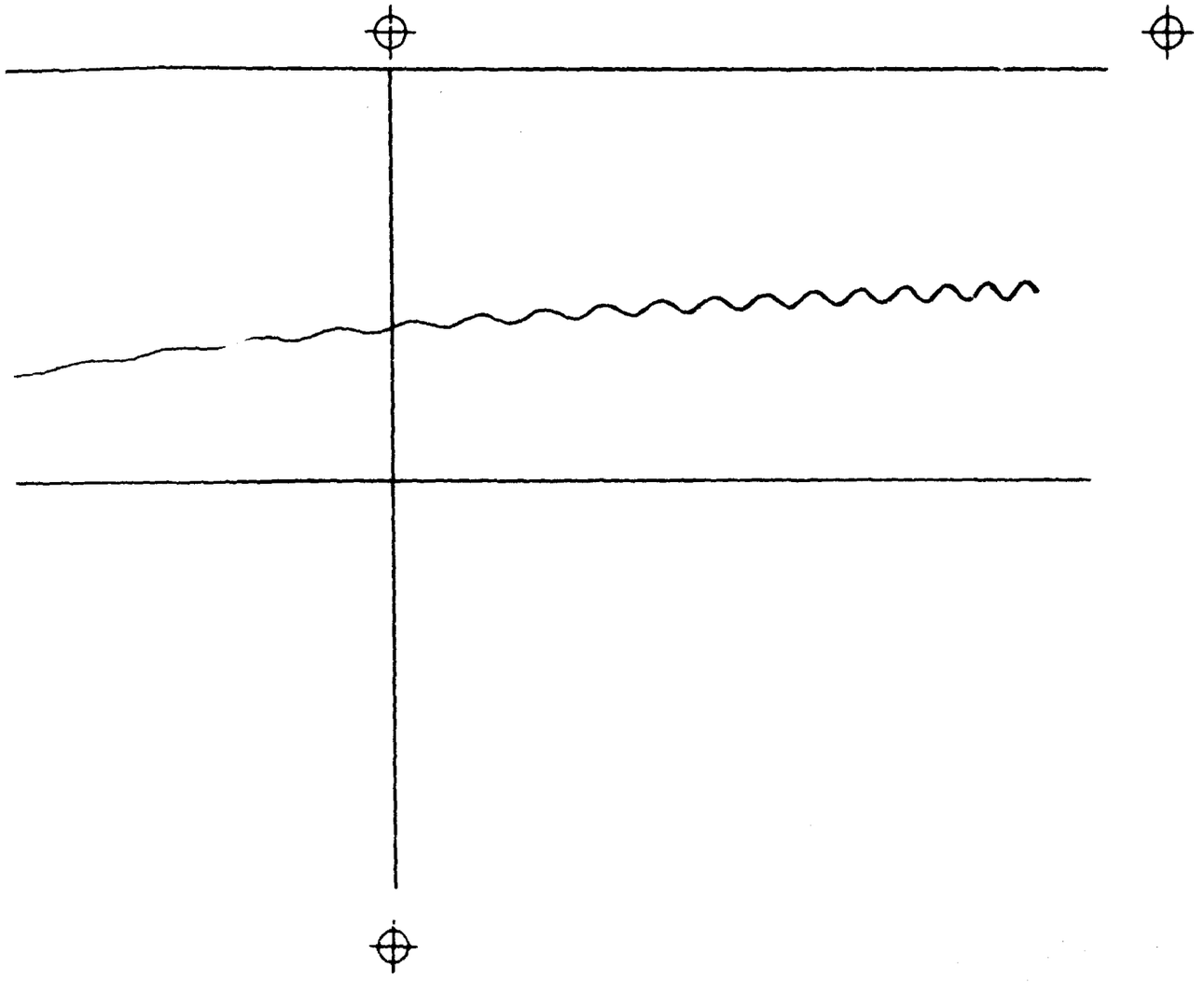

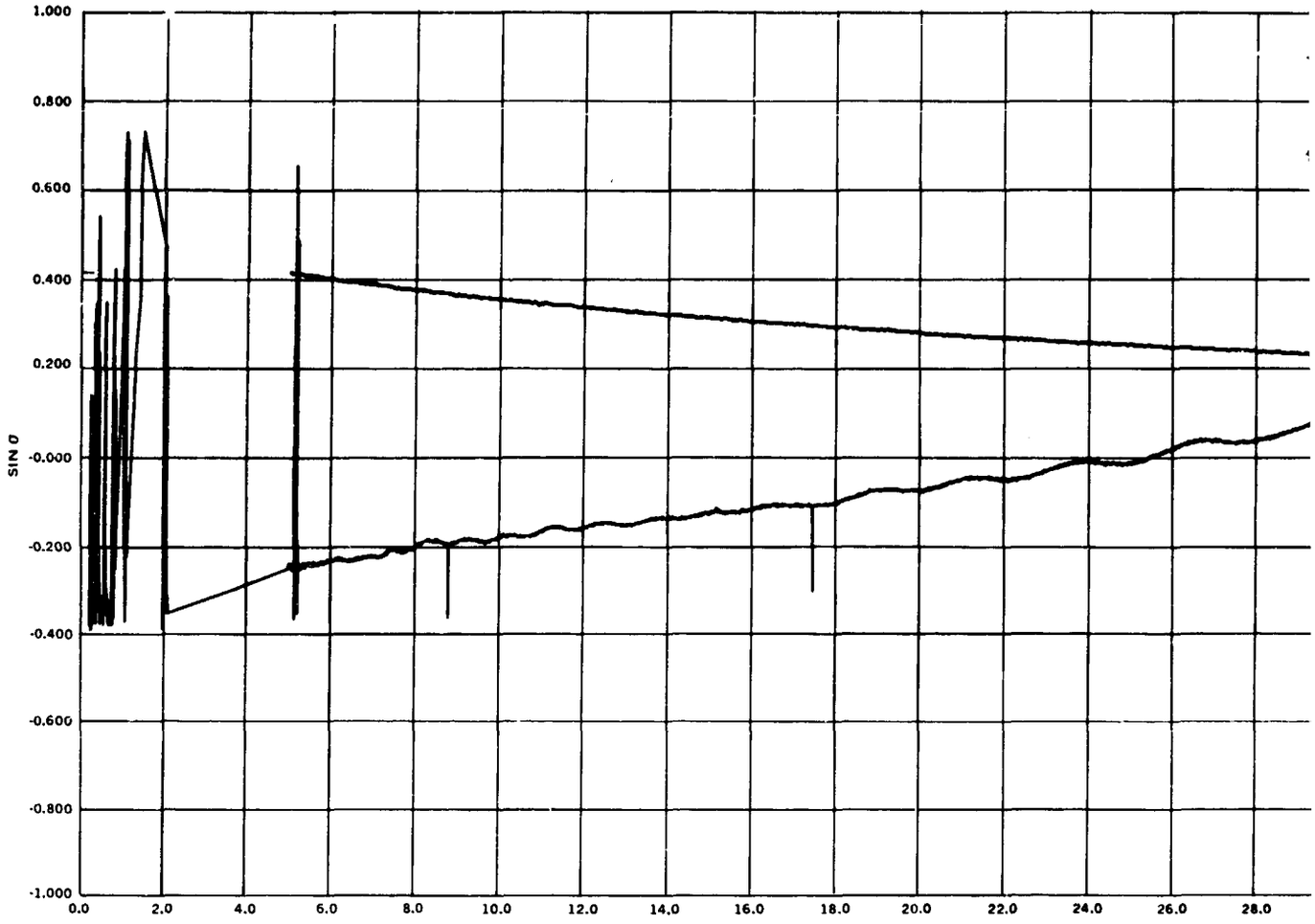

PLATE VI. (C
C. Yaw sor
E. Comput

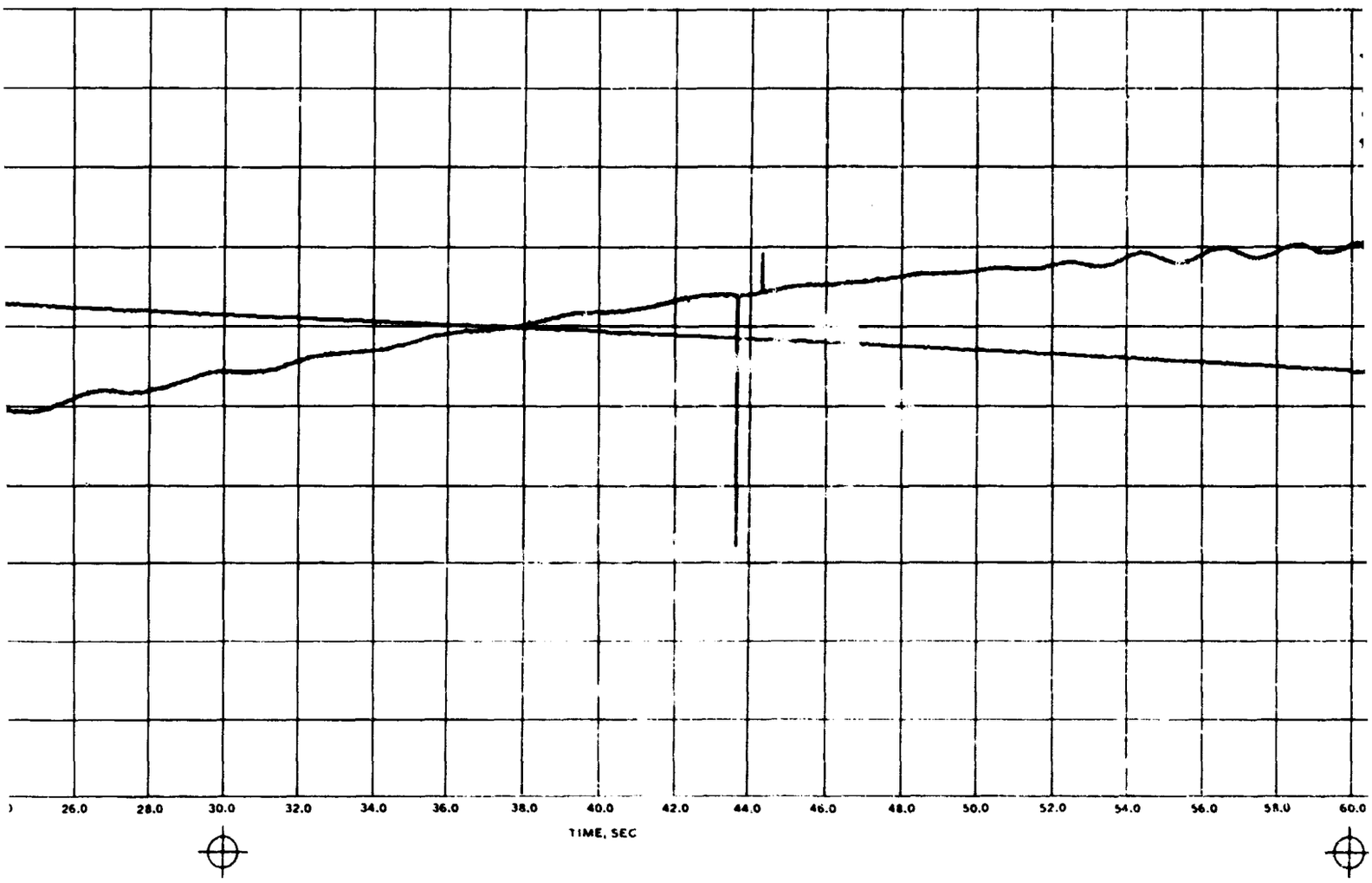

C.

PLATE VI. (Contd.)

C. Yaw sonde record.

E. Computer simulation of yaw sonde record; projectile not disturbed, but has increased magnus moment.

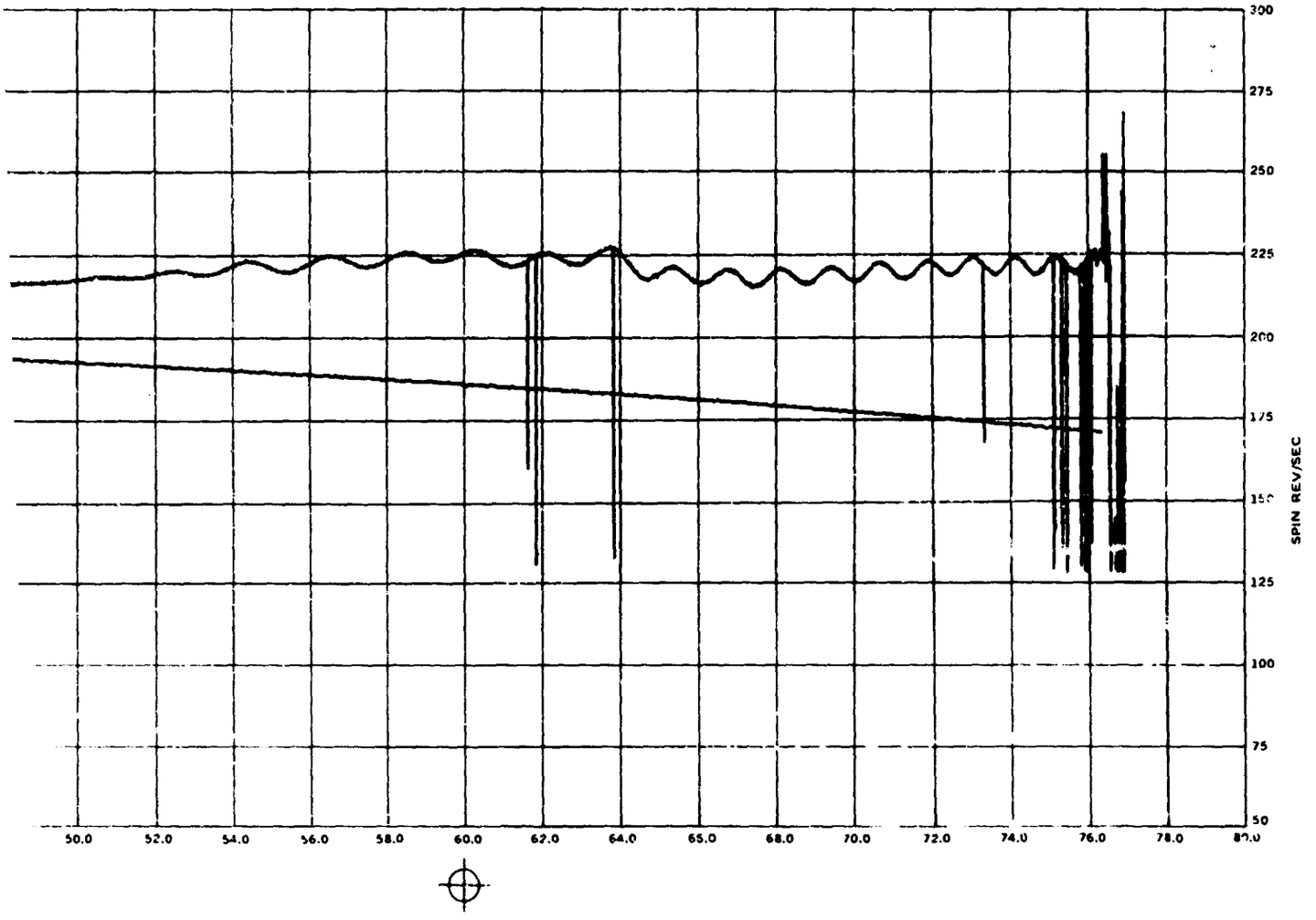
300
275
250
225
200
175
150
125
100
75
50
SPIN REV/SEC
50.0
52.0
54.0
56.0
58.0
60.0
62.0
64.0
65.0
68.0
70.0
72.0
74.0
76.0
78.0

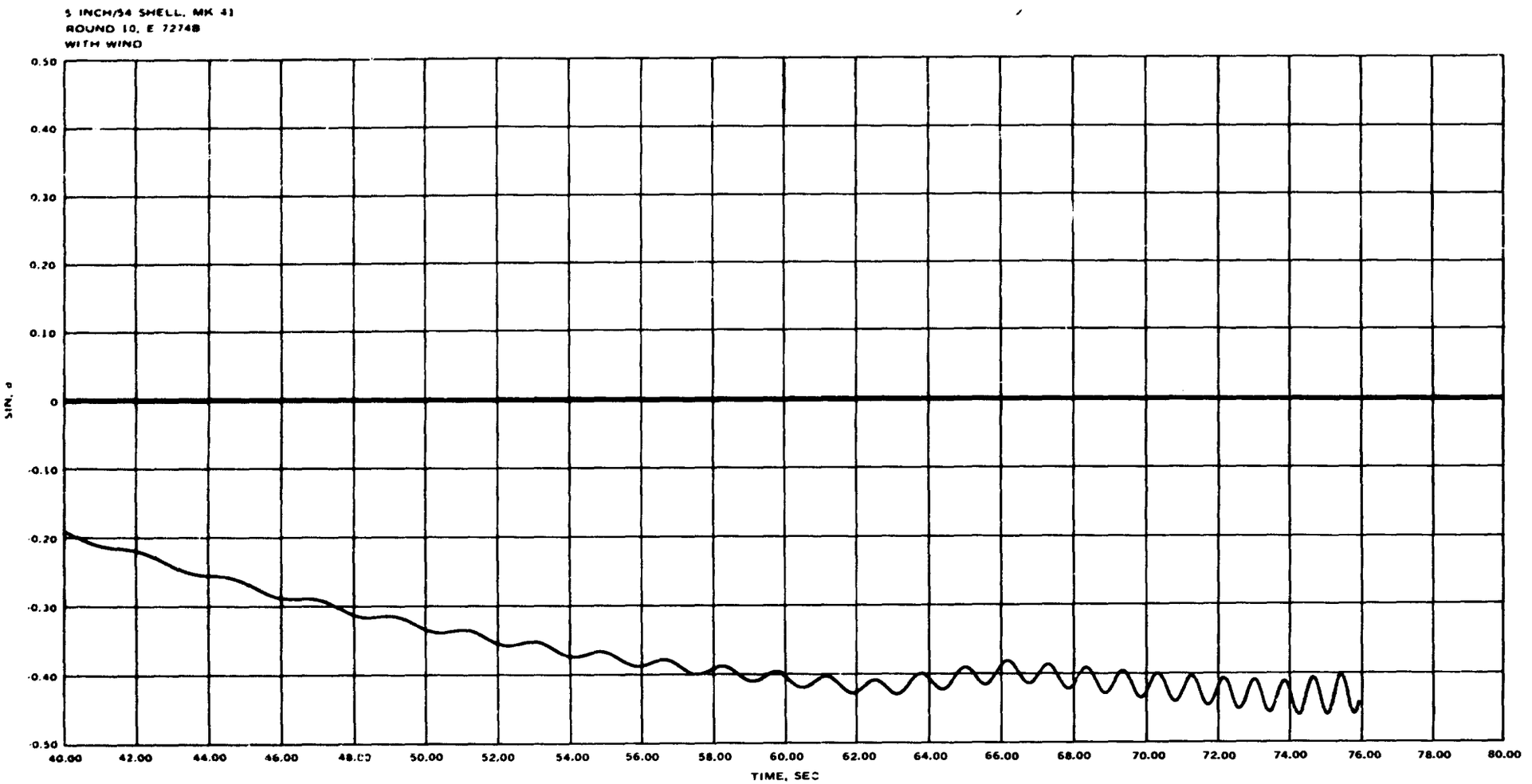

PLATE VII. Computed Yaw Sonde Curve for E-7274B, Round 10, Showing Effect of Wind Shear.

NOMENCLATURE

A	Dimensionless open decay coefficient
A_S	Azimuth of sun, measured from line of fire
a	Velocity of sound
$C_{subscript}$	Coefficient, aerodynamic notation
D	Dimensionless drag coefficient
d_s	Diameter
E_s	Elevation of sun
$F_{subscript}$	Force component
G_1	Dimensionless longitudinal gravity component
G_2	Dimensionless transverse gravity component
g	Acceleration of gravity (scalar)
H	Dimensionless yaw damping coefficient
I_p	Polar moment of inertia
I_T	Transverse moment of inertia
i	The unit imaginary
$K_{subscript}$	coefficient, ballistic notation
L = N-D	Dimensionless left coefficient
M	Dimensionless overturning moment coefficient
$M_{subscript}$	Moment component
m	Mass
N	Dimensionless normal force coefficient

n	Spin rate (rev/sec)
$p = 2\pi n$	Axial angular velocity component
$Q = \frac{1}{2}\rho V^2$	Dynamic pressure component
q	Horizontal angular pressure component
r	Third angular pressure component
$S = \pi d^2/4$	Area
T	Dimensionless Magnus moment coefficient
t	Time
$U = V/d$	Dimensionless velocity
u	Axial velocity component
V	Total velocity
v	Horizontal velocity component
w	Third velocity component
x	Horizontal distance along firing line
y	Altitude
α	Particle trajectory angle
γ	ℓn decrement of air density
$\delta = \phi - \theta$	Complex yaw angle
$\theta = \theta_2 + i\vartheta$	Complex trajectory deviation angle
$\mu = V/a$	Mach number
ρ	Air density
σ	Orientation angle referred to sun
$\phi = \phi_2 + i\phi_3$	Orientation deviation angle

REFERENCES

1. Ballistic Research Laboratories. The Aerodynamic Properties of the 105-mm HE Shell, M1, in Subsonic and Transonic Flight, by Eugene T. Roecker, Aberdeen Proving Ground, Md., BRL, September 1955. (BRL Memo Report No. 929).

2. U. S. Naval Ordnance Test Station. The Aerodynamic Characteristics of the 5-Inch High-Capacity Projectile Mk 41, Mod 0, by Eldon Dunn, China Lake, Calif., NOTS, February 1956. (NAVORD Report 5023, NOTS TP 1362).

3. Naval Weapons Laboratory. Dynamic Stability of the 5-Inch/54 Rocket Assisted Projectile (The Influence of a Nonlinear Magnus Moment), by W. R. Chadwick and J. F. Sylvester, Dahlgren, Va., NWL, October 1966. (NWL Technical Report No. 2059).

4. Davis, L., Jr., Follin, J. W., Jr., and L. Blitzer. Exterior Ballistics of Rockets. New York, Van Nostrand, 1958.

5. Royal Armament Research and Development Establishment. Yaw Measurement Analysis, by H. G. Haden, Woolwich, London, England, RARDE, December 1964. (RARDE Memorandum 54/64).

6. Ballistic Research Laboratories. The Aerodynamic Properties of the 155-mm Shell M101 from Free Flight Range Tests of Full Scale and 1/12 Scale Models, by B. G. Karpov and L. E. Schmidt (revised by K. Krial and L. C. MacAllister), Aberdeen Proving Ground, Md., BRL, June 1964. (BRL Memo Report No. 1582).

7. U. S. Naval Ordnance Test Station. Yawing of Bomroc, by W. R. Haseltine, China Lake, Calif., NOTS, September 1965 and December 1965. (NOTS Technical Notes 507-14 and 507-15).

8. "Letter Symbols for Aeronautical Sciences," in ASA Y10.7-1954. New York, American Society of Mechanical Engineers, 1954.

9. U. S. Naval Ordnance Test Station. The Drag Coefficient of the 5-Inch High Capacity Projectile Mk 41 Mod 0, by E. C. Barkofsky, China Lake, Calif., Nots, June 1955. (NAVORD Report 3503, NOTS TP 1132).

UNCLASSIFIED
Security Classification

DOCUMENT CONTROL DATA - R & D

(Security classification of title, body of abstract and indexing annotation must be entered when the overall report is classified)

1. ORIGINATING ACTIVITY *(Corporate author)*
Naval Weapons Center
China Lake, California 93555

2a. REPORT SECURITY CLASSIFICATION
UNCLASSIFIED

2b. GROUP

3. REPORT TITLE
YAWING MOTION OF 5"0 MK 41 PROJECTILE STUDIED BY MEANS OF YAW SONDES

4. DESCRIPTIVE NOTES *(Type of report and inclusive dates)*
Final Report

5. AUTHOR(S) *(First name, middle initial, last name)*
Haseltine, W. R.

6. REPORT DATE	7a. TOTAL NO. OF PAGES	7b. NO. OF REFS
August 1969	47	9

8a. CONTRACT OR GRANT NO.	9a. ORIGINATOR'S REPORT NUMBER(S)
b. PROJECT NO. Independent Exploratory Development Task R361-00-000/216-1/F008-98-16	NWC TP 4779
c. NOSC Tasks ORD-035-101/200-1/UF008-09-01 and ORD-351-001/200-1/UF17-323-501	9b. OTHER REPORT NO(S) *(Any other numbers that may be assigned this report)*
d.	

10. DISTRIBUTION STATEMENT
This document is subject to special export controls and each transmittal to foreign government or foreign nationals may be made only with prior approval of the Naval Weapons Center.

11. SUPPLEMENTARY NOTES	12. SPONSORING MILITARY ACTIVITY
	Naval Ordnance Systems Command Washington, D. C. 20360

13. ABSTRACT

The 5"0 Mk 41 projectile was fired at both high and low muzzle velocities, and its oscillatory yawing motion studied by a telemetry technique. At high subsonic velocities this projectile develops a steady precessional motion of amplitude about 4 degrees. On a long flight, from high velocity launch, this behavior shows up late on the downward trajectory leg. The instability at small yaw and the limit cycle were found to be caused by a large and highly nonlinear Magnus moment. Aerodynamic coefficients were derived.

DD FORM 1 NOV 65 1473 (PAGE 1)
S/N 0101-807-6801

UNCLASSIFIED
Security Classification

14. KEY WORDS	LINK A		LINK B		LINK C	
	ROLE	WT	ROLE	WT	ROLE	WT
Shell stability Magnus moment Limit cycles of artillery shell						